

An Extended Mathematical Model of the p53 Network: Simulating DNA Damage Responses Across Diverse Cellular Phenotypes

Tomáš Preisler

June 23, 2025

Abstract

The tumor suppressor protein p53 is a critical regulator of cellular responses to stress, particularly DNA damage. Its activation can lead to cell cycle arrest, DNA repair, senescence, or apoptosis, thus maintaining genomic integrity. Mathematical modeling has been instrumental in understanding the complex dynamics of the p53-Mdm2 feedback loop and its downstream pathways. This study presents an extended ordinary differential equation (ODE)-based model of the p53 network. The model incorporates key upstream kinases ATM and ATR, activated by different types of DNA damage (double strand breaks and single strand breaks / stalled replication forks, respectively) and downstream targets of p53 that include p21 (cell cycle arrest), Wip1 (feedback regulation), and a generic pro-apoptotic factor. A significant extension of this work involves the parameterization of the model to simulate a diverse array of cellular phenotypes, including normal differentiated cells (fibroblasts, hepatocytes, neurons, melanocytes), immune cells (monocytes), stem cells, senescent cells, UV-resistant cells, radioresistant cancer cells, and cancer cells with varying mutational statuses of p53. By adjusting kinetic parameters related to protein synthesis, degradation, interaction affinities, and damage repair capacities, the model qualitatively reproduces expected differential responses to DNA damaging agents such as IR and UV radiation in these cell types. This framework provides a versatile platform for exploring how cell-specific contexts modulate the dynamics of the p53 pathway and influence cell fate decisions, offering potential insights into tissue-specific cancer susceptibility and therapeutic responses.

Keywords: p53, Mdm2, ATM, ATR, response to DNA damage, mathematical modeling, cell cycle arrest, apoptosis, cell type specificity, cancer biology.

1 Introduction

The p53 protein, often termed the "guardian of the genome," plays a central role in the prevention of cancer by orchestrating cellular responses to a variety of stresses, most notably DNA damage [1, 2]. Upon activation, p53 functions as a transcription factor, inducing a wide range of target genes involved in cell cycle arrest, DNA repair, senescence, and apoptosis [3]. The decision between these outcomes is critical and context-dependent, influenced by the type and extent of damage, the cellular microenvironment, and the type of cell itself.

The core of the p53 regulatory network involves a negative feedback loop with its E3 ubiquitin ligase, Mdm2. Under normal and unstressed conditions, Mdm2 targets p53 for proteasomal degradation, keeping p53 levels low. Following DNA damage, p53 is stabilized and activated, mainly through post-translational modifications mediated by upstream kinases such as Ataxia Telangiectasia Mutated (ATM) and ATM and Rad3 related (ATR) [4, 5]. Activated p53 then transcribes Mdm2, reestablishing negative feedback, which can lead to oscillations in p53 levels observed experimentally [6, 7].

Mathematical modeling has proven invaluable in dissecting the intricacies of the p53 network, explaining its oscillatory behavior, and predicting cell fate decisions [8, 9]. Previous models have often focused on a generic mammalian cell or specific aspects of the pathway. However, the response to p53 activation varies significantly between different cell types and in pathological states like cancer.

This study aims to build on existing p53 models by:

1. Developing an extended ordinary differential equation (ODE) model that explicitly includes ATM and ATR activation by distinct DNA damage types (double-strand breaks from ionizing radiation (IR) and single-strand breaks/stalled forks from ultraviolet (UV) radiation).
2. Incorporating key p53 target genes: *CDKN1A* (encoding p21) for cell cycle arrest, *PPM1D* (encoding Wip1) for feedback regulation of ATM/ATR and p53, and a generic pro-apoptotic factor representing proteins such as Bax, Puma, or Noxa.
3. Systematically varying model parameters to simulate and explore DNA damage response dynamics in a wide range of distinct cellular phenotypes, reflecting their known biological characteristics.

The overarching goal is to create a more comprehensive and versatile in silico tool to investigate how cell-specific alterations in components of the p53 network influence cellular responses to genotoxic stress.

2 Model Description

The previous model described by Ciliberto, Novak, and Tyson in their 2005 paper, "Steady States and Oscillations in the p53/Mdm2 Network" [9], can be found in Appendix C.

The model is constructed as a system of coupled ordinary differential equations (ODEs) that describe the temporal dynamics of key protein concentrations and DNA damage levels. It integrates several interconnected modules.

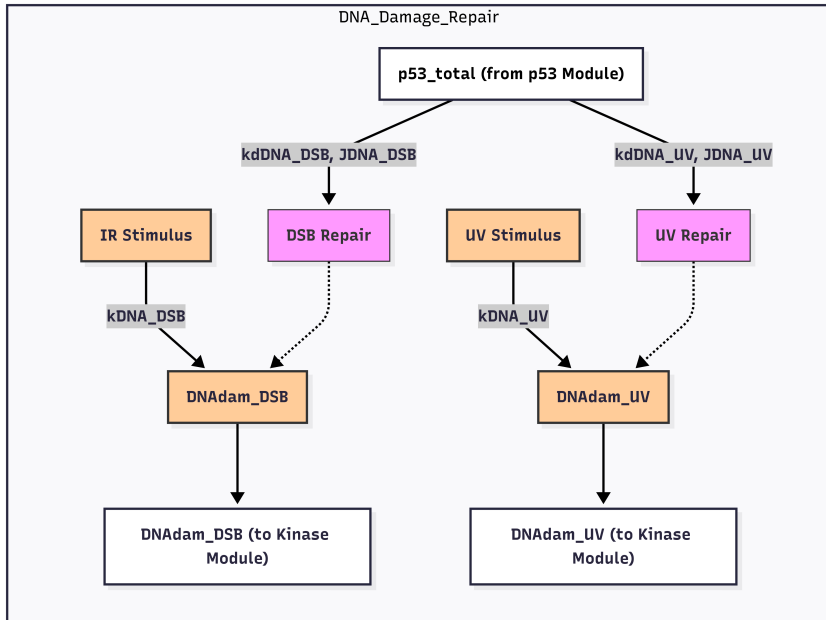


Figure 1: DNA Damage and Repair Module. IR and UV stimuli generate DNAAdam_DSB and DNAAdam_UV, respectively. p53_total promotes the repair of both damage types.

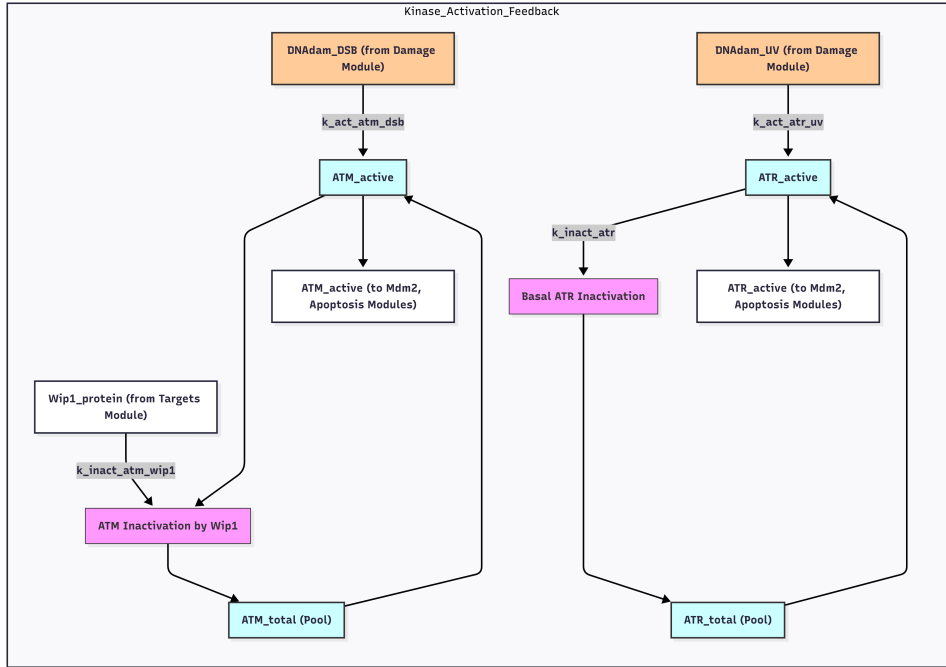


Figure 2: Kinase Activation and Feedback Module. DNAAdam_DS_B activates ATM, and DNAAdam_UV activates ATR. Wip1_protein, a p53 target, inactivates ATM_active. Active kinases are inputs to other modules.

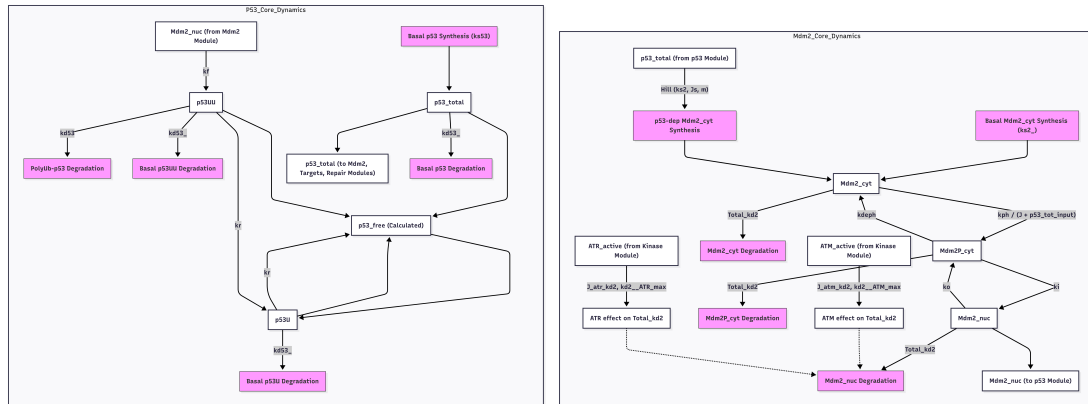


Figure 3: Core p53-Mdm2 Regulatory Module. (A) p53 synthesis, ubiquitination by Mdm2_nuc, and degradation. (B) Mdm2 synthesis (basal and p53-dependent), phosphorylation, nucleocytoplasmic shuttling, and degradation influenced by ATM/ATR.

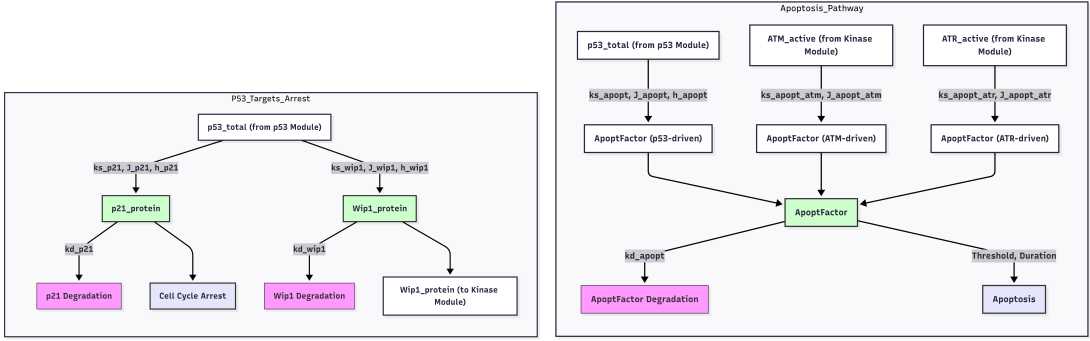


Figure 4: p53 Target Genes and Cellular Outcomes. (A) p53_Total induces p21_Protein (leading to Cell Cycle Arrest) and Wip1_Protein (feedback to Kinase Module). (B) ApoptFactor synthesis is driven by p53_Total, ATM_Active, and ATR_Active, potentially leading to Apoptosis if a threshold and duration are met.

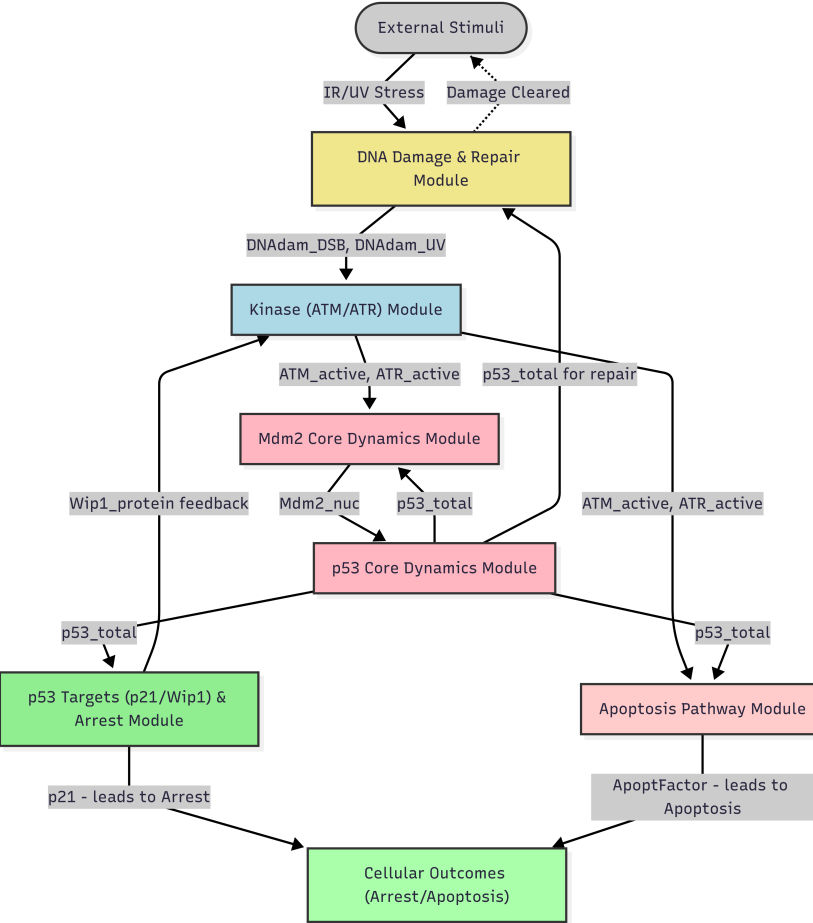


Figure 5: Integrated model of the p53 DNA damage response pathway. External stimuli trigger the DNA Damage & Repair Module, which activates the Kinase Module. Kinases and p53_Total influence the Mdm2 Core Dynamics and p53 Core Dynamics. p53_Total drives the p53 Targets and Apoptosis Pathway modules, leading to cellular outcomes like Arrest or Apoptosis.

The complete mathematical formulation of the model, detailing the ODEs for each species, is provided in Appendix A.1.

3 Modeled Genes and Their Roles in the Network

The model incorporates several key proteins central to the p53 pathway. In the following, we describe each gene product, its biological function, and how this function is represented within the mathematical model.

p53 (TP53)

Biological Function: A tumor suppressor protein that acts as a transcription factor, activated in response to cellular stresses such as DNA damage, oncogene activation, and hypoxia. Activated p53 regulates genes involved in cell cycle arrest, apoptosis, DNA repair, and senescence, thus preventing the proliferation of damaged cells [1, 10]. **Model Representation:** $[p53_{tot}]$ represents the total cellular concentration of p53. Its synthesis is modeled as a constant rate (k_{s53}). Its degradation is twofold: a basal Mdm2-independent degradation (k'_{d53}) and an ubiquitination-dependent Mdm2-dependent degradation. Nuclear Mdm2 ($[Mdm2_{nuc}]$) binds to free p53 ($[p53_{free}]$) at a rate k_f to form a monoubiquitinated complex ($[p53U]$), which can then be further ubiquitinated by $[Mdm2_{nuc}]$ to $[p53UU]$. $[p53UU]$ is then degraded at rate k_{d53} . DNA damage-activated kinases ATM and ATR stabilize p53 primarily by inhibiting the k_f interaction (parameter $K_{inhibit,kf,atm}$, $K_{inhibit,kf,atr}$ in code, implicitly modeled if k_f becomes kinase-dependent) and / or by promoting Mdm2 degradation (see Mdm2 section). Activated $[p53_{tot}]$ then drives the transcription of Mdm2, p21, Wip1, and ApoptFactor through Hill-type functions, representing its role as a transcriptional activator.

Mdm2 (MDM2)

Biological Function: The primary negative regulator of p53. It is an E3 ubiquitin ligase that targets p53 for proteasomal degradation. Mdm2 is also a direct transcriptional target of p53, forming a tightly regulated negative feedback loop crucial for controlling p53 levels and activity [11, 12]. The activity and localization of Mdm2 are also regulated by phosphorylation, for example, by ATM and Akt.

Model Representation: The model tracks cytoplasmic Mdm2 ($[Mdm2_{cyt}]$), phosphorylated cytoplasmic Mdm2 ($[Mdm2P_{cyt}]$) and nuclear Mdm2 ($[Mdm2_{nuc}]$). $[Mdm2_{cyt}]$ synthesis includes a basal rate (k'_{s2}) and a Hill-type function dependent on p53 (rate k_{s2} , Hill coefficient m , saturation constant J_s), reflecting its transcriptional up-regulation by p53. Cytoplasmic Mdm2 can be phosphorylated by p53-related stress signals (rate k_{ph} , dependent on $[p53_{tot}]$ via saturation constant J) to $[Mdm2P_{cyt}]$, which can be dephosphorylated (k_{deph}). $[Mdm2P_{cyt}]$ translocates to the nucleus (rate k_i) to become $[Mdm2_{nuc}]$, which can shuttle back to the cytoplasm (rate k_o). The nuclear-cytoplasmic volume ratio is V_{ratio} . $[Mdm2_{nuc}]$ is responsible for the ubiquitination of p53. Its degradation rate ($k_{d2,eff}$) is increased by active ATM ($k_{d2,ATM,max}$, $J_{atm,kd2}$) and ATR ($k_{d2,ATR,max}$, $J_{atr,kd2}$), representing a mechanism for stabilization of p53 after DNA damage [13].

ATM (Ataxia Telangiectasia Mutated)

Biological Function: A serine/threonine kinase that is a master regulator of the DNA double-strand break (DSB) response. Upon activation by DSBs, ATM phosphorylates a vast array of substrates, including p53 (enhancing its stability and activity), Mdm2 (inhibiting its interaction with p53 and promoting its degradation), Chk2 (another kinase that amplifies the signal), and H2AX (a histone variant marking damage sites) [5].

Model Representation: $[ATM_{active}]$ represents the active form of ATM. Its activation is proportional to the amount of DSB damage ($[DNAAdam_{DSB}]$) and the available inactive ATM (total ATM $[ATM_{total}]$ minus $[ATM_{active}]$), with an activation rate constant $k_{act,atm,dsb}$. Active

ATM is inactivated by Wip1 ($[Wip1_{protein}]$) at a rate $k_{inact,atm,wip1}$. $[ATM_{active}]$ contributes to p53 stabilization by enhancing Mdm2_nuc degradation and, in this model, can also directly promote $[ApoptFactor]$ synthesis (rate $k_{s,apopt,atm}$, saturation $J_{apopt,atm}$).

ATR (ATM and Rad3-related)

Biological Function: Another PI3K-like serine/threonine kinase that responds primarily to single-strand DNA (ssDNA) regions, often arising from UV damage, stalled replication forks, or processed DSBs. ATR, often in conjunction with its partner ATRIP, activates downstream effectors like Chk1 and p53 to initiate cell cycle arrest and DNA repair [14].

Model Representation: $[ATR_{active}]$ represents the active form of ATR. Its activation is proportional to UV-induced damage ($[DNAdam_{UV}]$) and available inactive ATR (total ATR $[ATR_{total}]$ minus $[ATR_{active}]$), with a rate constant $k_{act,atr,uv}$. $[ATR_{active}]$ undergoes basal inactivation (rate $k_{inact,atr}$). Similar to ATM, $[ATR_{active}]$ contributes to p53 stabilization by enhancing $[Mdm2_{nuc}]$ degradation and can directly promote $[ApoptFactor]$ synthesis (rate $k_{s,apopt,atr}$, saturation $J_{apopt,atr}$).

p21 (CDKN1A, WAF1/CIP1)

Biological Function: A potent cyclin-dependent kinase (CDK) inhibitor. As a primary transcriptional target of p53, p21 plays a crucial role in mediating p53-dependent cell cycle arrest, primarily at G1/S and G2/M transitions, providing time for DNA repair [15, 16].

Model Representation: $[p21_{protein}]$ synthesis is modeled as a Hill function dependent on $[p53_{tot}]$ (rate $k_{s,p21}$, Hill coefficient h_{p21} , saturation constant J_{p21}). It undergoes basal degradation (rate $k_{d,p21}$). Elevated levels of $[p21_{protein}]$ are interpreted as an indicator of cell cycle arrest.

Wip1 (PPM1D)

Biological Function: A serine/threonine phosphatase (type 2C) that is a transcriptional target of p53. Wip1 plays a critical role in the negative feedback regulation of the DNA damage response by dephosphorylating and inactivating key DDR proteins, including ATM, ATR, Chk1, Chk2, and p53 itself. This helps to terminate the DDR signaling once damage is resolved [17, 18].

Model Representation: $[Wip1_{protein}]$ synthesis is modeled as a Hill function dependent on $[p53_{tot}]$ (rate $k_{s,wip1}$, Hill coefficient h_{wip1} , saturation constant J_{wip1}). It undergoes basal degradation (rate $k_{d,wip1}$). In this model, its primary role is the inactivation of $[ATM_{active}]$.

ApoptFactor

Biological Function: This is a generic variable representing the collective activity of various pro-apoptotic proteins whose expression or activation is promoted by p53 (e.g., Bax, Noxa, Puma) or directly by ATM/ATR signaling. Accumulation of these factors leads to the activation of the caspase cascade and programmed cell death [19–21].

Model Representation: $[ApoptFactor]$ synthesis is driven by three components: p53-dependent synthesis (Hill function: rate $k_{s,apopt}$, Hill coefficient h_{apopt} , saturation J_{apopt}), ATM-dependent synthesis (Michaelis-Menten: rate $k_{s,apopt,atm}$, saturation $J_{apopt,atm}$), and ATR-dependent synthesis (Michaelis-Menten: rate $k_{s,apopt,atr}$, saturation $J_{apopt,atr}$). It undergoes basal degradation (rate $k_{d,apopt}$). If $[ApoptFactor]$ levels exceed a certain $ApoptFactor_{threshold}$ for a minimum duration ($ApoptFactor_{duration,min}$), the cell is considered to have committed to apoptosis.

4 Simulation of Diverse Cellular Phenotypes

A key feature of this work is the adaptation of the core *AdvancedCell_Baseline* model to represent a variety of distinct mammalian cell types. This is achieved by systematically modifying specific kinetic parameters based on known biological characteristics and expected responses. Citations are provided to support the rationale where applicable.

- **AdvancedCell_Baseline:** *Rationale:* Represents a generic, healthy mammalian cell with typical p53 dynamics and responses. Parameters are often derived from foundational p53 modeling studies [6, 7] or adjusted to produce characteristic p53 oscillations and dose-dependent responses to damage.

Key Parameters: Standard literature-derived or fitted values for p53-Mdm2 loop, kinase activation, and downstream target induction.

- **UVResistantCell:** *Rationale:* Cells adapted to or inherently better at handling UV radiation, such as melanocytes or cells with highly efficient Nucleotide Excision Repair (NER).

Key Parameter Changes & Justification:

- $k_{dDNA,UV}$ (increased): Reflects enhanced NER capacity [22].
- $k_{act,atr,uv}$ (increased): Faster and more robust ATR activation due to efficient damage recognition.
- $k_{d2,ATR,max}$ (increased): Stronger ATR-mediated Mdm2 degradation ensures p53 can be stabilized effectively for repair or apoptosis if damage is overwhelming.
- $ApoptFactor_{threshold}$ (increased): Cells might tolerate more damage or require stronger pro-apoptotic signals if they are highly proficient at repair.

- **RadioresistantCancerCell_p53wt:** *Rationale:* Cancer cells can develop resistance to radiotherapy (IR) through various mechanisms even with wild-type p53, such as enhanced DNA repair or altered apoptotic signaling [23].

Key Parameter Changes & Justification:

- $k_{dDNA,DSB}$ (increased): Reflects enhanced DSB repair capacity (e.g., upregulated NHEJ or HR pathways).
- $ApoptFactor_{threshold}$ (increased), $k_{s,apopt}/k_{s,apopt,atm}$ (reduced): Represents acquired apoptosis resistance, possibly due to overexpression of anti-apoptotic proteins (e.g., Bcl-2 family members) or defects in apoptotic execution pathways, common in cancer [24].
- $k_{s,p21}$ (increased), J_{p21} (decreased sensitivity): Robust p21 induction might favor arrest and repair over apoptosis, contributing to resistance.

- **FibroblastCell:** *Rationale:* Differentiated stromal cells, often quiescent. They need effective DDR to maintain tissue integrity.

Key Parameter Changes & Justification:

- $p21_{G1,arrest,threshold}$ (lower), $k_{s,p21}$ (slightly increased): Fibroblasts readily undergo cell cycle arrest in response to damage [25].
- Apoptosis parameters ($ApoptFactor_{threshold}$, etc.) set for moderate sensitivity, as fibroblasts can undergo apoptosis but also senescence upon persistent damage.

- **HepatocyteCell:** *Rationale:* Metabolically active cells in the liver with significant regenerative capacity. They require robust repair but must also control proliferation and eliminate severely damaged cells.

Key Parameter Changes & Justification:

- $k_{dDNA,DSB}/k_{dDNA,UV}$ (increased): Hepatocytes are exposed to various genotoxins and need efficient repair [26].
 - $ApoptFactor_{threshold}$ (somewhat higher): To prevent excessive cell loss during normal function or minor stress, given their regenerative role.
 - $k_{d,p21}$ (increased, i.e., p21 less stable): Allows for more transient arrest, facilitating return to proliferation for regeneration once damage is repaired [27].
- **NeuronCell:** *Rationale:* Post-mitotic cells; p53's role is primarily in deciding between survival (promoting repair/neuroprotection) and apoptosis, rather than cell cycle control via p21 [28].
- Key Parameter Changes & Justification:*
- $k_{s,p21}$ (drastically reduced): Reflects the post-mitotic state where p21-mediated cell cycle arrest is not a primary outcome.
 - $ApoptFactor_{threshold}$ (lower), $k_{s,apopt}$ (higher): Neurons can be sensitive to certain types of damage, and p53 can drive apoptosis to remove dysfunctional cells [29]. Kinase-driven apoptosis ($k_{s,apopt,atm/atr}$) might be more prominent.
- **MelanocyteCell:** *Rationale:* Skin cells responsible for melanin production, constantly exposed to UV. They have specialized UV protection and response mechanisms.
- Key Parameter Changes & Justification:*
- $k_{act,atr,uv}$ (increased), ATR_{total} (increased): Reflects a highly responsive ATR pathway to UV damage [30].
 - $k_{dDNA,UV}$ (increased): Efficient repair of UV photoproducts is crucial.
 - $p53_{thresh,apopt,UV}$ (lower): May be more sensitive to UV-induced apoptosis to prevent accumulation of mutations.
 - $DNAAdam_{UV,necro,thresh}$ (lower): High UV doses can lead to necrosis (sunburn).
- **MonocyteCell:** *Rationale:* Immune cells that patrol tissues, can differentiate, and must respond to damage or infection.
- Key Parameter Changes & Justification:*
- $k_{act,atm,dsb}/k_{act,atr,uv}$ (increased): Robust kinase activation for rapid response.
 - $k_{d2,ATM,max}/k_{d2,ATR,max}$ (increased): Efficient p53 stabilization.
 - $k_{s,p21}$ (increased): Monocytes are often in G0/G1 and can efficiently arrest.
 - $k_{s,apopt,atm}/k_{s,apopt,atr}$ (increased): Kinase-driven apoptosis might be important for eliminating infected or severely damaged monocytes [31].
- **CancerCell_p53Mutant:** *Rationale:* Represents over 50% of human cancers where p53 is mutated, typically losing its ability to transactivate target genes [32].
- Key Parameter Changes & Justification:*
- $k_{s2}, k_{s,p21}, k_{s,wip1}, k_{s,apopt}$ (drastically reduced): Reflects loss of p53's transcriptional activity for its key targets, leading to uncontrolled proliferation and apoptosis resistance.
- **CancerCell_Restored_p53:** *Rationale:* Simulates therapeutic approaches aiming to reactivate mutant p53 or restore its pathways [33].
- Key Parameter Changes & Justification:*
- $k_{s2}, k_{s,p21}, k_{s,wip1}, k_{s,apopt}$ (partially increased from mutant state): Represents partial restoration of p53's transcriptional function.

- Apoptosis thresholds adjusted to be more sensitive than the full mutant but potentially still more resistant than a normal cell due to other acquired cancer mutations.
- **StemCell_Embryonic:** *Rationale:* Embryonic stem cells (ESCs) have a very low tolerance for DNA damage to preserve genomic integrity for development, often favoring apoptosis over repair for significant lesions [20, 21].
Key Parameter Changes & Justification:
 - $ApoptFactor_{threshold}$ (very low), $k_{s,apopt}$ (high), J_{apopt} (sensitive): Parameters set for a highly sensitive and potent apoptotic response.
 - $K_{inhibit,kf,atm/atr}$ (stronger), $k_{d2,ATM/ATR,max}$ (stronger): Rapid and robust p53 stabilization.
 - $k_{s,p21}$ (lower or less stable): Less emphasis on prolonged arrest; apoptosis is preferred.
- **SenescentCell:** *Rationale:* Cells in a state of stable cell cycle arrest, often resistant to apoptosis, contributing to aging and age-related diseases [34].
Key Parameter Changes & Justification:
 - $k_{s,p21}$ (high), $k_{d,p21}$ (low): Reflects high, stable levels of p21 contributing to irreversible arrest (though p16, not in this model, is also key).
 - $k_{s,apopt}$ (very low), $ApoptFactor_{threshold}$ (very high): Represents the characteristic apoptosis resistance of senescent cells (SASP factors, not modeled, can contribute).

5 Simulation Setup and Illustrative Results

Simulations are performed using Python with SciPy’s `solve_ivp` to integrate the ODEs defined in `p53_full_system` (Appendix A.1). Initial conditions represent a basal, unstressed state. DNA damage (IR or UV) is applied as specified by `BasicEnvironment` or `AdvancedEnvironment` parameters. The figures below illustrate typical dynamic responses for selected cell types under a simulated IR pulse (e.g., from `AdvancedEnvironment` with $ampl_{IR} = 1.0$ for 10 min, then $ampl_{IR} = 0$).

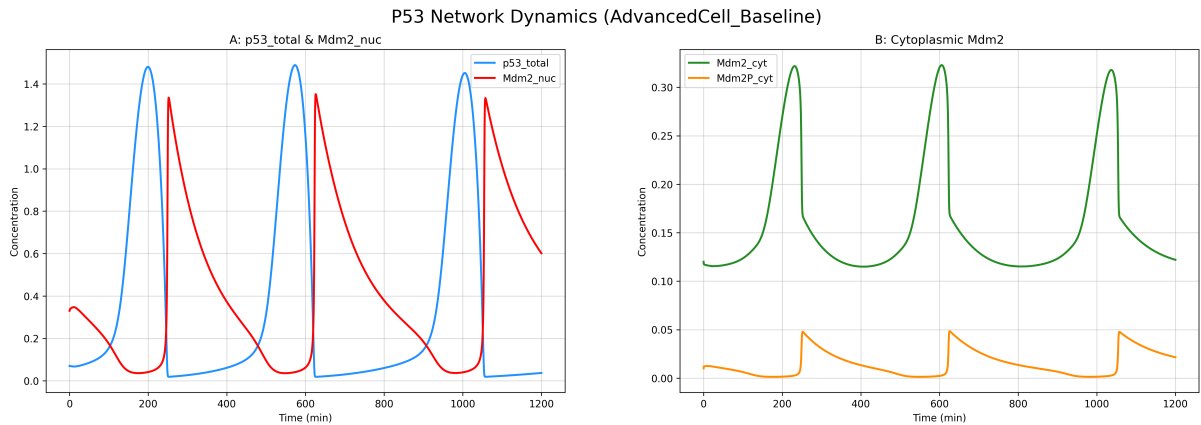


Figure 6: Baseline Response of `AdvancedCell_Baseline` to IR. (A) `p53_total` (blue) exhibits oscillations, driving oscillations in `Mdm2_nuc` (red). (B) Cytoplasmic `Mdm2` species also oscillate.

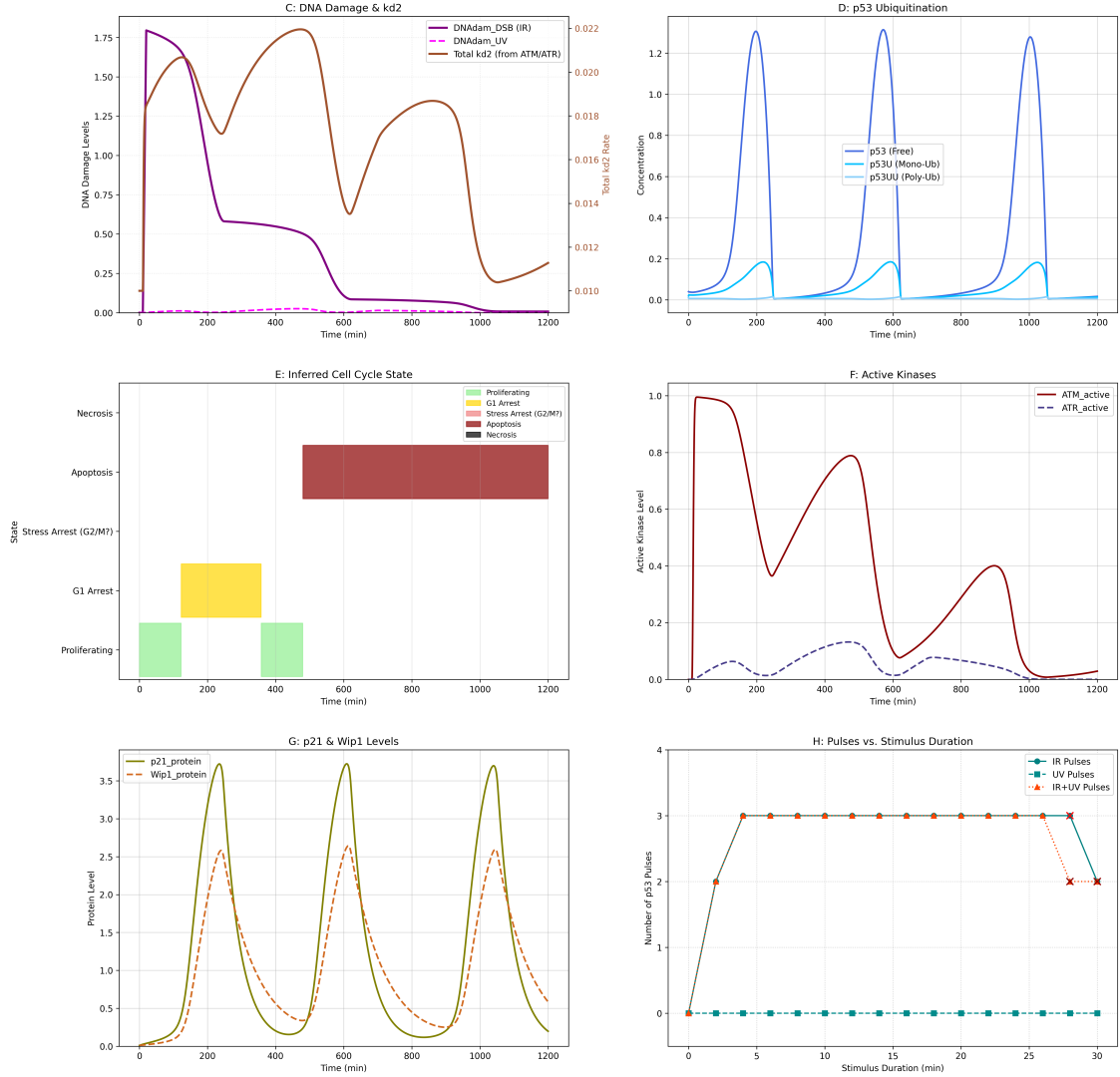


Figure 7: (C) DNAAdam_DSB (brown) is induced and gradually repaired, while Total_kd2 (purple) shows transient increases due to ATM/ATR activation. (D) p53 ubiquitinated forms follow p53_total dynamics. (E) The cell undergoes G1 Arrest (yellow) and apoptosis due to p21 induction. (F) ATM_active (red) shows a strong initial peak followed by damped oscillations. (G) p21_protein (green) and Wip1_protein (orange) are induced in pulses. (H) Number of p53 peaks (pulses) by time under IR/UV pulses

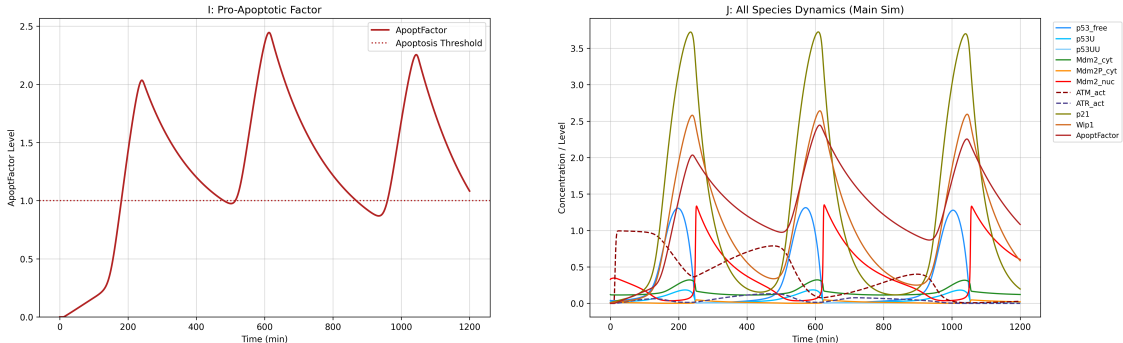


Figure 8: (I) ApoptFactor (red) rises with p53 pulses and crosses the apoptosis threshold (dotted red) for this damage level, indicating apoptosis. (J) All species together in one graph

Interpretation: This represents a robust baseline response in a healthy cell, where the oscillations of p53 drive the pulses of p21 leading to cell cycle arrest, allowing time for DNA repair. Wip1 contributes to the negative feedback. Apoptosis is a possible outcome if the damage is severe or persistent.

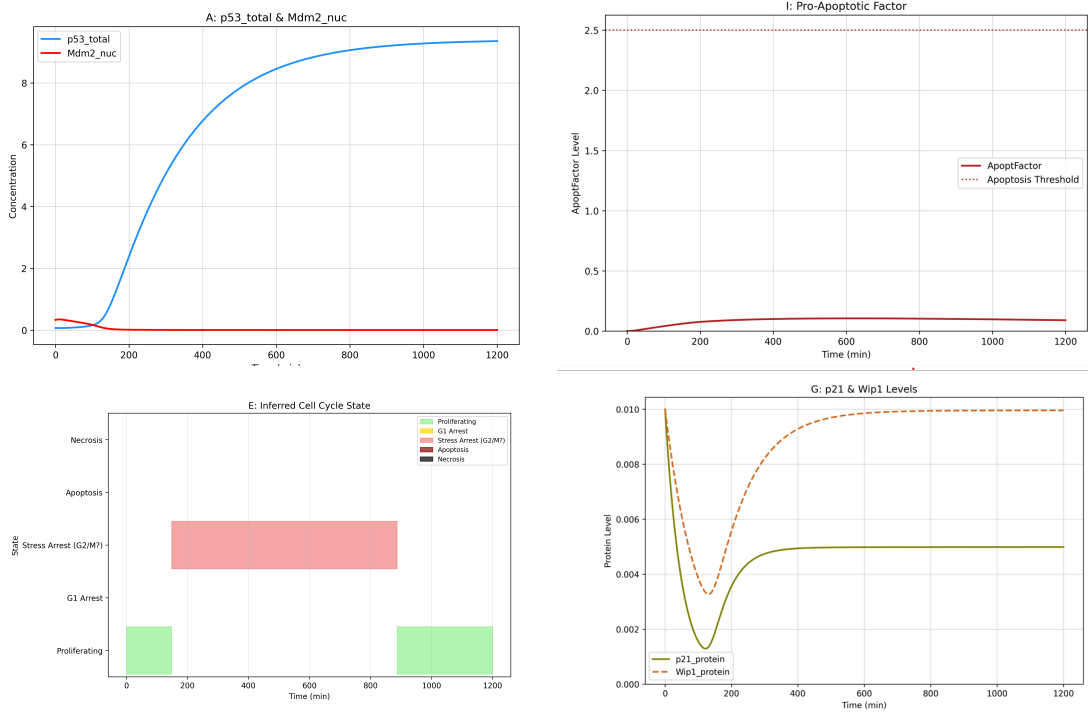


Figure 9: Apoptosis Resistance in CancerCell_p53Mutant to IR. (A) If p53 is synthesized but non-functional, p53_total (blue) might accumulate but fails to effectively induce Mdm2_nuc (red). (G) p21_protein (green) and Wip1_protein (orange) levels remain very low. (I) Consequently, ApoptFactor (red) synthesis is minimal and does not approach the apoptosis threshold. (E) The cell remains in a "Proliferating" state despite the damage.

Interpretation: This highlights the consequence of p53 mutation. The loss of p53's transcriptional activity prevents the induction of key downstream effectors like p21 and pro-apoptotic factors, leading to a failure to arrest or undergo apoptosis, a hallmark of many cancers.

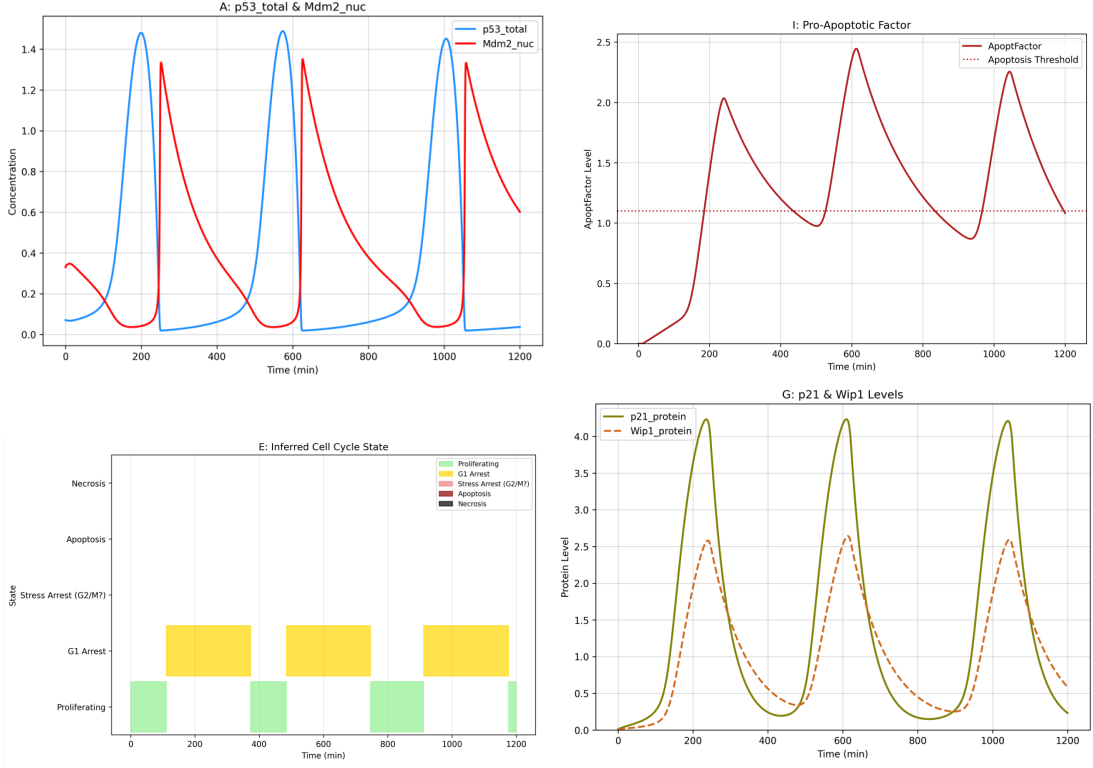


Figure 10: Sustained Arrest in FibroblastCell to IR. (A, G) $p53_total$ induces strong and sustained pulses of $p21_protein$. (E) This leads to a prolonged G1 Arrest state (yellow). (I) ApoptFactor levels rise but remain below the apoptosis threshold, indicating that the cell prioritizes arrest and repair.

Interpretation: Fibroblasts often opt for robust cell cycle arrest to allow ample time for DNA repair. While apoptosis is possible with severe damage, parameters are tuned such that $p21$ -mediated arrest is a prominent and sustained outcome for moderate damage levels.

All other studied cells can be found in the appendix.

6 Discussion

This study presents an extended mathematical model of the $p53$ network, incorporating distinct DNA damage inputs (DSB and SSB/UV-type), key upstream kinases (ATM/ATR), and critical downstream effectors ($p21$, Wip1, ApoptFactor). A novel aspect of this work is the systematic parameterization to simulate a diverse array of cellular phenotypes. By adjusting parameters reflecting known biological differences in protein expression, activity, or repair capacities, the model aims to capture the varied ways different cell types respond to genotoxic stress via the $p53$ pathway.

The ability to model multiple cell types provides a powerful tool for comparative systems biology. For instance, comparing a `CancerCell_p53Mutant` with an `AdvancedCell_Baseline` can highlight the direct consequences of $p53$ inactivation on cell fate decisions. Simulating a `CancerCell_Restored_p53` allows for in silico exploration of $p53$ -reactivating therapies and potential resistance mechanisms that might persist. The `StemCell_Embryonic` model, with its bias towards apoptosis, underscores the stringent quality control mechanisms in cells critical for development. Conversely, the `SenescentCell` model reflects the apoptosis resistance often observed in these arrested cells. The specialized cell types like `MelanocyteCell` or `RadioresistantCancerCell` allow investigation into mechanisms conferring resistance to specific damaging agents.

The inclusion of both ATM and ATR, activated by different damage types, allows for more

nuanced simulations of responses to complex genotoxic environments where cells might encounter mixed types of DNA lesions or different types of therapeutic agents (e.g., IR vs. UV-mimetic drugs). The explicit modeling of p21, Wip1, and a generic ApoptFactor allows for a clearer interpretation of cellular outcomes like arrest or apoptosis commitment.

Limitations

Despite its extended scope, the model has limitations.

1. **Simplification:** Many pathway components and regulatory interactions are still simplified or omitted for tractability (e.g., detailed p53 post-translational modifications, specific apoptotic proteins, other Mdm2 family members like MdmX, explicit DNA repair pathways, interaction with NF- κ B or metabolic pathways).
2. **Parameter Values:** While parameter changes for different cell types are biologically motivated, many are qualitative estimations rather than directly fitted experimental data for each specific cell type and interaction. Obtaining comprehensive, quantitative parameter sets for each cell type is a major challenge.
3. **Spatial Aspects:** The model is based on ODEs, assuming well-mixed compartments, and does not capture spatial heterogeneities within the cell or nucleus.
4. **Cellular Outcomes:** The interpretation of "arrest" and "apoptosis" is based on thresholds for p21 and ApoptFactor, which is a simplification of complex biological decision-making processes. Senescence entry is not dynamically modeled but rather represented by a parameter set for an already senescent cell.

Future Work

Future extensions could include:

1. Incorporating more detailed DNA repair pathways (e.g., NHEJ, HR, NER, BER).
2. Adding other p53 target genes and interacting pathways (e.g., autophagy, metabolism, specific caspases).
3. Systematic parameter fitting and validation against experimental data from specific cell types under defined damage conditions.
4. Integrating the model with data on gene expression or protein levels from different tissues or cancer types to personalize predictions.

7 Conclusion

The extended mathematical model of the p53 network presented here offers a flexible framework for studying DNA damage responses. Its ability to simulate diverse cellular phenotypes by adjusting a rationalized set of parameters provides a valuable platform for generating hypotheses about cell-type-specific sensitivities to DNA damaging agents, mechanisms of drug resistance in cancer, and the fundamental principles governing cell fate decisions. This work underscores the importance of cellular context in shaping the outcomes of p53 activation and provides a foundation for more detailed and predictive models of this critical tumor suppressor pathway.

References

1. Levine, A. J. P53, the Cellular Gatekeeper for Growth and Division. *Cell* (1997).
2. Vogelstein, B., Lane, D. P. & Levine, A. J. Surfing the p53 network. *Nature* (2000).
3. Harris, S. L. & Levine, A. J. The p53 pathway: positive and negative feedback loops. *Oncogene* (2005).
4. Shiloh, Y. & Ziv, Y. The ATM protein kinase: regulating the cellular response to genotoxic stress, and more. *Nature Reviews Molecular Cell Biology* (2013).
5. Shiloh, Y. ATM and related protein kinases: safeguarding genome integrity. *Nature Reviews Cancer* (2003).
6. Lahav, G. *et al.* Dynamics of the p53-Mdm2 feedback loop in individual cells. *Nature Genetics* (2004).
7. Ma, L. *et al.* A plausible model for the digital response of p53 to DNA damage. *Proceedings of the National Academy of Sciences of the United States of America* (2005).
8. Zhang, X., Liu, F. & Wang, W. Two-phase dynamics of p53 in the DNA damage response. *Proceedings of the National Academy of Sciences of the United States of America* (2011).
9. Ciliberto, A., Novak, B. & Tyson, J. J. Steady States and Oscillations in the p53/Mdm2 Network. *Cell Cycle* **4**, 488–493. (2005) (Feb. 2005).
10. Vousden, K. H. & Prives, C. Blinded by the Light: The Growing Complexity of p53. *Cell* (2009).
11. Momand, J., Zambetti, G. P., Olson, D. C., George, D. L. & Levine, A. J. The mdm-2 oncogene product forms a complex with the p53 protein and inhibits p53-mediated transactivation. *Cell* (1992).
12. Barak, Y., Juven, T., Haffner, R. & Oren, M. Mdm2 expression is induced by wild type p53 activity. *The EMBO Journal* (1993).
13. Meek, D. W. & Knippschild, U. Posttranslational modification of MDM2. *Molecular Cancer Research* (2003).
14. Cimprich, K. A. & Cortez, D. ATR: an essential regulator of genome integrity. *Nature Reviews Molecular Cell Biology* (2008).
15. El-Deiry, W. S. *et al.* WAF1, a potential mediator of p53 tumor suppression. *Cell* (1993).
16. Harper, J. W., Adami, G. R., Wei, N., Keyomarsi, K. & Elledge, S. J. The p21 Cdk-interacting protein Cip1 is a potent inhibitor of G1 cyclin-dependent kinases. *Cell* (1993).
17. Lu, X. *et al.* The p53-Induced Oncogenic Phosphatase PPM1D Interacts with Uracil DNA Glycosylase and Suppresses Base Excision Repair. *Molecular Cell* (2004).
18. Shreeram, S. *et al.* Wip1 Phosphatase Modulates ATM-Dependent Signaling Pathways. *Molecular Cell* (2006).
19. Fridman, J. S. & Lowe, S. W. Control of apoptosis by p53. *Oncogene* (2003).
20. Roos, W. P. & Kaina, B. DNA damage-induced cell death by apoptosis. *Trends in Molecular Medicine* (2006).
21. Roos, W. P., Thomas, A. D. & Kaina, B. DNA damage and the balance between survival and death in cancer biology. *Nature Reviews Cancer* (2016).
22. Friedberg, E. C., Walker, G. C. & Siede, W. DNA Repair and Mutagenesis. *null* (2006).
23. Begg, A. C., Stewart, F. A. & Vens, C. Strategies to improve radiotherapy with targeted drugs. *Nature Reviews Cancer* (2011).

24. Fulda, S. Tumor resistance to apoptosis. *International Journal of Cancer* (2009).
25. Leonardo, A. D., Linke, S. P., Clarkin, K. C. & Wahl, G. M. DNA damage triggers a prolonged p53-dependent G1 arrest and long-term induction of Cip1 in normal human fibroblasts. *Genes & Development* (1994).
26. Carr, M. I. & Jones, S. N. Regulation of the Mdm2-p53 signaling axis in the DNA damage response and tumorigenesis. *Translational cancer research* (2016).
27. Seki, E., Albrecht, J. H., Meyer, A. H. & Hu, M. Y. Regulation of cyclin-dependent kinase inhibitor p21(WAF1/Cip1/Sdi1) gene expression in hepatic regeneration. *Hepatology* (1997).
28. Miller, F. D. & Kaplan, D. R. Neurotrophin signalling pathways regulating neuronal apoptosis. *Cellular and Molecular Life Sciences* (2001).
29. Morrison, R. S. & Kinoshita, Y. The role of p53 in neuronal cell death. *Cell Death & Differentiation* (2000).
30. Brash, D. E. UV signature mutations. *Photochemistry and Photobiology* (2015).
31. Gudkov, A. V. & Komarova, E. A. The role of p53 in determining sensitivity to radiotherapy. *Nature Reviews Cancer* (2003).
32. Hollstein, M. C., Sidransky, D., Vogelstein, B. & Harris, C. C. P53 mutations in human cancers. *Science* (1991).
33. Bykov, V. J. N., Eriksson, S., Bianchi, J. & Wiman, K. G. Targeting mutant p53 for efficient cancer therapy. *Nature Reviews Cancer* (2018).
34. Childs, B. G., Durik, M., Baker, D. J. & van Deursen, J. M. Cellular senescence in aging and age-related disease: from mechanisms to therapy. *Nature Medicine* (2015).

A Model Equations for the Extended p53 System

Let species concentrations be denoted by square brackets, e.g., $[p53_{\text{tot}}]$. Let ϵ represent a small positive constant (e.g., 10^{-9}) added to denominators to prevent division by zero.

Species

- $[p53_{\text{tot}}]$: Total p53 protein
- $[p53U]$: Mono-ubiquitinated p53
- $[p53UU]$: Di-ubiquitinated p53
- $[Mdm2_{\text{cyt}}]$: Cytoplasmic Mdm2
- $[Mdm2P_{\text{cyt}}]$: Phosphorylated cytoplasmic Mdm2
- $[Mdm2_{\text{nuc}}]$: Nuclear Mdm2
- $[DNAAdam_{\text{DSB}}]$: DNA double-strand breaks
- $[DNAAdam_{\text{UV}}]$: DNA damage from UV
- $[ATM_{\text{active}}]$: Active ATM kinase
- $[ATR_{\text{active}}]$: Active ATR kinase
- $[p21_{\text{protein}}]$: p21 protein
- $[Wip1_{\text{protein}}]$: Wip1 protein
- $[ApoptFactor]$: Generic Pro-Apoptotic Factor

Intermediate Definitions

1. Free p53:

$$[p53_{\text{free}}] = \max(0, [p53_{\text{tot}}] - ([p53U] + [p53UU])) \quad (1)$$

2. Input Signals (Time-dependent):

$$IR_{\text{signal}}(t) = \begin{cases} ampl_{\text{IR}} & \text{if } IR_{\text{start}} < t < IR_{\text{end}} \\ 0 & \text{otherwise} \end{cases} \quad (2)$$

$$UV_{\text{signal}}(t) = \begin{cases} ampl_{\text{UV}} & \text{if } UV_{\text{start}} < t < UV_{\text{end}} \\ 0 & \text{otherwise} \end{cases} \quad (3)$$

3. Effective Mdm2 Nuclear Degradation Rate ($k_{d2,\text{eff}}$):

$$\begin{aligned} k_{d2,\text{eff}} = k'_{d2} + & \left(k_{d2,\text{ATM,max}} \frac{[ATM_{\text{active}}]}{J_{\text{atm},kd2} + [ATM_{\text{active}}] + \epsilon} \right) \\ & + \left(k_{d2,\text{ATR,max}} \frac{[ATR_{\text{active}}]}{J_{\text{atr},kd2} + [ATR_{\text{active}}] + \epsilon} \right) \end{aligned} \quad (4)$$

(Note: k'_{d2} is the basal degradation rate p['kd2_'] from the code.)

4. Effective p53-Mdm2 Binding Rate:

$$k_{f,\text{eff}} = k_f \quad (5)$$

5. p53-dependent Mdm2 Synthesis Term:

$$S_{Mdm2,p53} = k_{s2} \frac{[p53_{\text{tot}}]^m}{J_s^m + [p53_{\text{tot}}]^m + \epsilon} \quad (6)$$

6. Mdm2 Phosphorylation Term:

$$Phos_{Mdm2} = \frac{k_{ph}}{J + [p53_{\text{tot}}] + \epsilon} [Mdm2_{\text{cyt}}] \quad (7)$$

7. DNA Repair Terms:

$$R_{\text{DSB}} = k_{dDNA, \text{DSB}} [p53_{\text{tot}}] \frac{[DNAAdam_{\text{DSB}}]}{J_{\text{DNA,DSB}} + [DNAAdam_{\text{DSB}}] + \epsilon} \quad (8)$$

$$R_{\text{UV}} = k_{dDNA, \text{UV}} [p53_{\text{tot}}] \frac{[DNAAdam_{\text{UV}}]}{J_{\text{DNA,UV}} + [DNAAdam_{\text{UV}}] + \epsilon} \quad (9)$$

8. p21 Synthesis Term:

$$S_{p21} = k_{s,p21} \frac{[p53_{\text{tot}}]^{h_{p21}}}{J_{p21}^{h_{p21}} + [p53_{\text{tot}}]^{h_{p21}} + \epsilon} \quad (10)$$

9. Wip1 Synthesis Term:

$$S_{Wip1} = k_{s,wip1} \frac{[p53_{\text{tot}}]^{h_{wip1}}}{J_{wip1}^{h_{wip1}} + [p53_{\text{tot}}]^{h_{wip1}} + \epsilon} \quad (11)$$

10. Apoptotic Factor Synthesis Terms:

$$S_{\text{Apopt,p53}} = k_{s,\text{apopt}} \frac{[p53_{\text{tot}}]^{h_{\text{apopt}}}}{J_{\text{apopt}}^{h_{\text{apopt}}} + [p53_{\text{tot}}]^{h_{\text{apopt}}} + \epsilon} \quad (12)$$

$$S_{\text{Apopt,ATM}} = k_{s,\text{apopt,atm}} \frac{[ATM_{\text{active}}]}{J_{\text{apopt,atm}} + [ATM_{\text{active}}] + \epsilon} \quad (13)$$

$$S_{\text{Apopt,ATR}} = k_{s,\text{apopt,atr}} \frac{[ATR_{\text{active}}]}{J_{\text{apopt,atr}} + [ATR_{\text{active}}] + \epsilon} \quad (14)$$

$$S_{\text{Apopt,total}} = S_{\text{Apopt,p53}} + S_{\text{Apopt,ATM}} + S_{\text{Apopt,ATR}} \quad (15)$$

System of Ordinary Differential Equations

$$\frac{d[p53_{\text{tot}}]}{dt} = k_{s53} - k'_{d53}[p53_{\text{tot}}] - k_{d53}[p53UU] \quad (16)$$

$$\begin{aligned} \frac{d[p53U]}{dt} &= k_{f,\text{eff}}[Mdm2_{\text{nuc}}][p53_{\text{free}}] + k_r[p53UU] \\ &\quad - [p53U](k_r + k_{f,\text{eff}}[Mdm2_{\text{nuc}}]) - k'_{d53}[p53U] \end{aligned} \quad (17)$$

$$\frac{d[p53UU]}{dt} = k_{f,\text{eff}}[Mdm2_{\text{nuc}}][p53U] - [p53UU](k_r + k'_{d53} + k_{d53}) \quad (18)$$

$$\frac{d[Mdm2_{\text{cyt}}]}{dt} = k'_{s2} + S_{Mdm2,p53} - k'_{d2}[Mdm2_{\text{cyt}}] + k_{deph}[Mdm2P_{\text{cyt}}] - Phos_{Mdm2} \quad (19)$$

$$\begin{aligned} \frac{d[Mdm2P_{\text{cyt}}]}{dt} &= Phos_{Mdm2} - k_{deph}[Mdm2P_{\text{cyt}}] - k_i[Mdm2P_{\text{cyt}}] \\ &\quad + k_o[Mdm2_{\text{nuc}}] - k'_{d2}[Mdm2P_{\text{cyt}}] \end{aligned} \quad (20)$$

$$\frac{d[Mdm2_{\text{nuc}}]}{dt} = V_{\text{ratio}}(k_i[Mdm2P_{\text{cyt}}] - k_o[Mdm2_{\text{nuc}}]) - k_{d2,\text{eff}}[Mdm2_{\text{nuc}}] \quad (21)$$

$$\frac{d[DNAAdam_{\text{DSB}}]}{dt} = k_{\text{DNA,DSB}} \cdot IR_{\text{signal}}(t) - R_{\text{DSB}} \quad (22)$$

$$\frac{d[DNAAdam_{\text{UV}}]}{dt} = k_{\text{DNA,UV}} \cdot UV_{\text{signal}}(t) - R_{\text{UV}} \quad (23)$$

$$\begin{aligned} \frac{d[ATM_{\text{active}}]}{dt} &= k_{\text{act,atm,dsb}}[DNAAdam_{\text{DSB}}]([ATM_{\text{total}}] - [ATM_{\text{active}}]) \\ &\quad - k_{\text{inact,atm,wip1}}[Wip1_{\text{protein}}][ATM_{\text{active}}] \end{aligned} \quad (24)$$

$$\frac{d[ATR_{\text{active}}]}{dt} = k_{\text{act,atr,uv}}[DNAAdam_{\text{UV}}]([ATR_{\text{total}}] - [ATR_{\text{active}}]) - k_{\text{inact,atr}}[ATR_{\text{active}}] \quad (25)$$

$$\frac{d[p21_{\text{protein}}]}{dt} = S_{p21} - k_{d,p21}[p21_{\text{protein}}] \quad (26)$$

$$\frac{d[Wip1_{\text{protein}}]}{dt} = S_{Wip1} - k_{d,wip1}[Wip1_{\text{protein}}] \quad (27)$$

$$\frac{d[ApoptFactor]}{dt} = S_{\text{Apopt,total}} - k_{d,\text{apopt}}[ApoptFactor] \quad (28)$$

Parameter Mapping for users (Python Code to LaTeX Symbol)

- $p['ks53'] \rightarrow k_{s53}$
- $p['kd53_'] \rightarrow k'_{d53}$ (basal p53 degradation)
- $p['kd53'] \rightarrow k_{d53}$ (Mdm2-mediated p53UU degradation)

- $p[{'kf'}] \rightarrow k_f$ (used in $k_{f,\text{eff}}$)
- $p[{'kr'}] \rightarrow k_r$
- $p[{'ks2_'}] \rightarrow k'_{s2}$ (basal Mdm2 synthesis rate)
- $p[{'ks2'}] \rightarrow k_{s2}$ (p53-dependent Mdm2 synthesis rate)
- $p[{'Js'}] \rightarrow J_s$ (Hill constant for Mdm2 synthesis by p53)
- $p[{'m'}] \rightarrow m$ (Hill coefficient for Mdm2 synthesis by p53)
- $p[{'kph'}] \rightarrow k_{ph}$ (Mdm2 phosphorylation rate)
- $p[{'J'}] \rightarrow J$ (Michaelis constant for Mdm2 phosphorylation denominator)
- $p[{'kdeph'}] \rightarrow k_{deph}$ (Mdm2P dephosphorylation rate)
- $p[{'Vratio'}] \rightarrow V_{\text{ratio}}$ (Cytoplasmic to Nuclear volume ratio)
- $p[{'ki'}] \rightarrow k_i$ (Mdm2P import rate to nucleus)
- $p[{'ko'}] \rightarrow k_o$ (Mdm2 export rate from nucleus)
- $p[{'kd2_'}] \rightarrow k'_{d2}$ (basal Mdm2 degradation rate for all Mdm2 forms; used in $k_{d2,\text{eff}}$)
- $p[{'J_atm_kd2'}] \rightarrow J_{\text{atm},kd2}$
- $p[{'kd2__ATM_max'}] \rightarrow k_{d2,\text{ATM,max}}$
- $p[{'J_atr_kd2'}] \rightarrow J_{\text{atr},kd2}$
- $p[{'kd2__ATR_max'}] \rightarrow k_{d2,\text{ATR,max}}$
- $p[{'kDNA_DSB'}] \rightarrow k_{\text{DNA,DSB}}$ (DSB formation rate per unit IR signal)
- $p[{'kdDNA_DSB'}] \rightarrow k_{d\text{DNA,DSB}}$ (DSB repair rate)
- $p[{'JDNA_DSB'}] \rightarrow J_{\text{DNA,DSB}}$ (Saturation constant for DSB repair)
- $p[{'kDNA_UV'}] \rightarrow k_{\text{DNA,UV}}$ (UV damage formation rate per unit UV signal)
- $p[{'kdDNA_UV'}] \rightarrow k_{d\text{DNA,UV}}$ (UV damage repair rate)
- $p[{'JDNA_UV'}] \rightarrow J_{\text{DNA,UV}}$ (Saturation constant for UV damage repair)
- $p[{'k_act_atm_dsb'}] \rightarrow k_{\text{act,atm,dsb}}$
- $p[{'ATM_total'}] \rightarrow [ATM_{\text{total}}]$
- $p[{'k_inact_atm_wip1'}] \rightarrow k_{\text{inact,atm,wip1}}$
- $p[{'k_act_atr_uv'}] \rightarrow k_{\text{act,atr,uv}}$
- $p[{'ATR_total'}] \rightarrow [ATR_{\text{total}}]$
- $p[{'k_inact_atr'}] \rightarrow k_{\text{inact,atr}}$
- $p[{'ks_p21'}] \rightarrow k_{s,p21}$
- $p[{'h_p21'}] \rightarrow h_{p21}$

- $p['J_p21'] \rightarrow J_{p21}$
- $p['kd_p21'] \rightarrow k_{d,p21}$
- $p['ks_wip1'] \rightarrow k_{s,wip1}$
- $p['h_wip1'] \rightarrow h_{wip1}$
- $p['J_wip1'] \rightarrow J_{wip1}$
- $p['kd_wip1'] \rightarrow k_{d,wip1}$
- $p['ks_apopt'] \rightarrow k_{s,apopt}$
- $p['h_apopt'] \rightarrow h_{apopt}$
- $p['J_apopt'] \rightarrow J_{apopt}$
- $p['ks_apopt_atm'] \rightarrow k_{s,apopt,atm}$
- $p['J_apopt_atm'] \rightarrow J_{apopt,atm}$
- $p['ks_apopt_atr'] \rightarrow k_{s,apopt,atr}$
- $p['J_apopt_atr'] \rightarrow J_{apopt,atr}$
- $p['kd_apopt'] \rightarrow k_{d,apopt}$
- $p.get('ampl_IR', 0.0) \rightarrow ampl_{IR}$
- $p.get('ampl_UV', 0.0) \rightarrow ampl_{UV}$
- $p.get('IR_start', -1) \rightarrow IR_{start}$
- $p.get('IR_end', -1) \rightarrow IR_{end}$
- $p.get('UV_start', -1) \rightarrow UV_{start}$
- $p.get('UV_end', -1) \rightarrow UV_{end}$

B Simulation results of all cell types

Simulations were performed using the environmental conditions specified in Table 1. The cellular parameters used correspond to those detailed for `AdvancedCell_Baseline` (Table 2) or the respective modifications for specialized cell types as outlined in Tables 3–13.

Parameter	Description	Value
UV_start	UV start time	10
UV_end	UV end time	700
ampl_UV	Amplitude of UV signal	0.001
IR_start	IR start time	10
IR_end	IR end time	20
ampl_IR	Amplitude of IR signal	1.0

Table 1: Parameters of the Environment

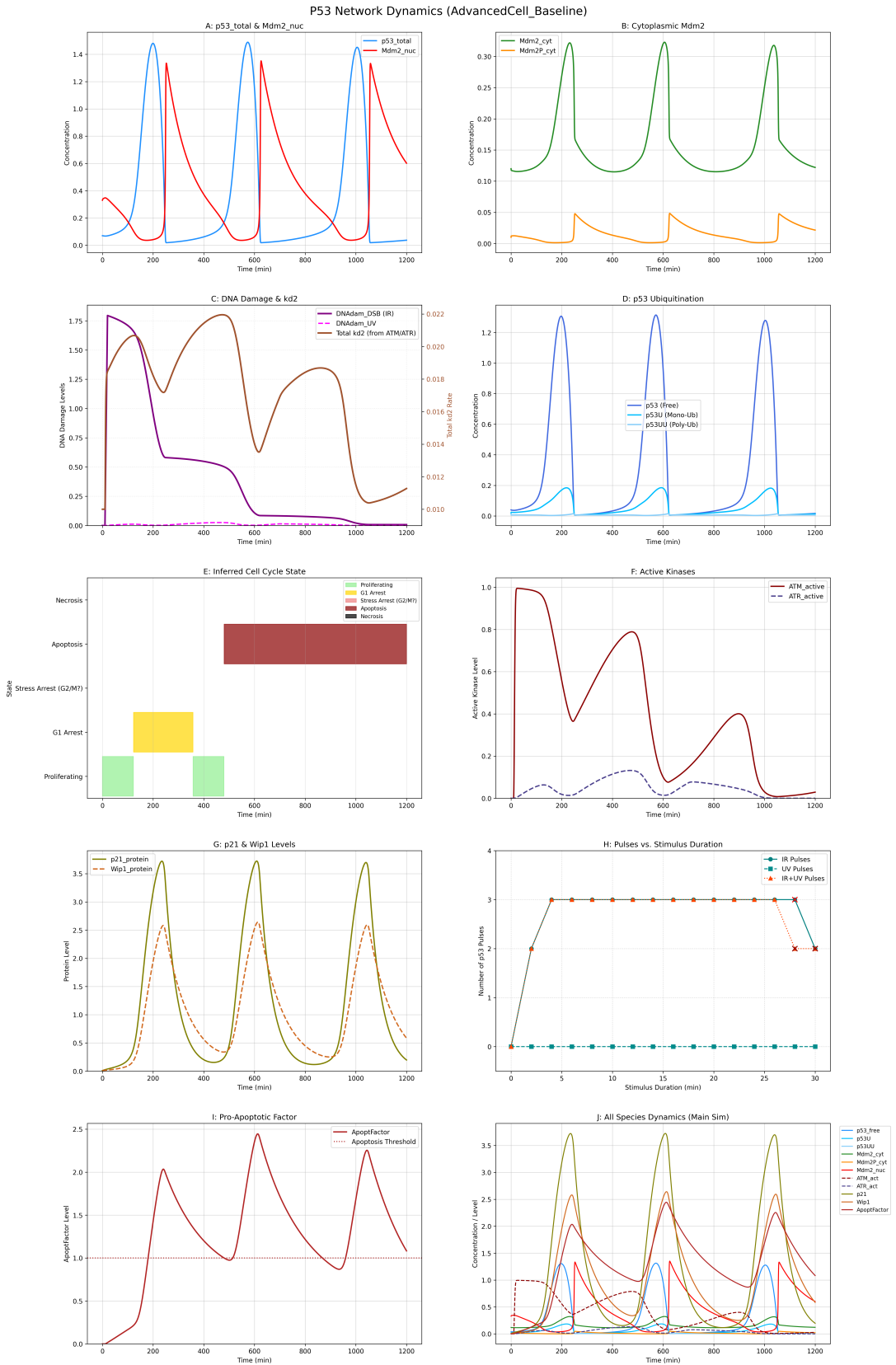


Figure 11: Advanced Cell baseline

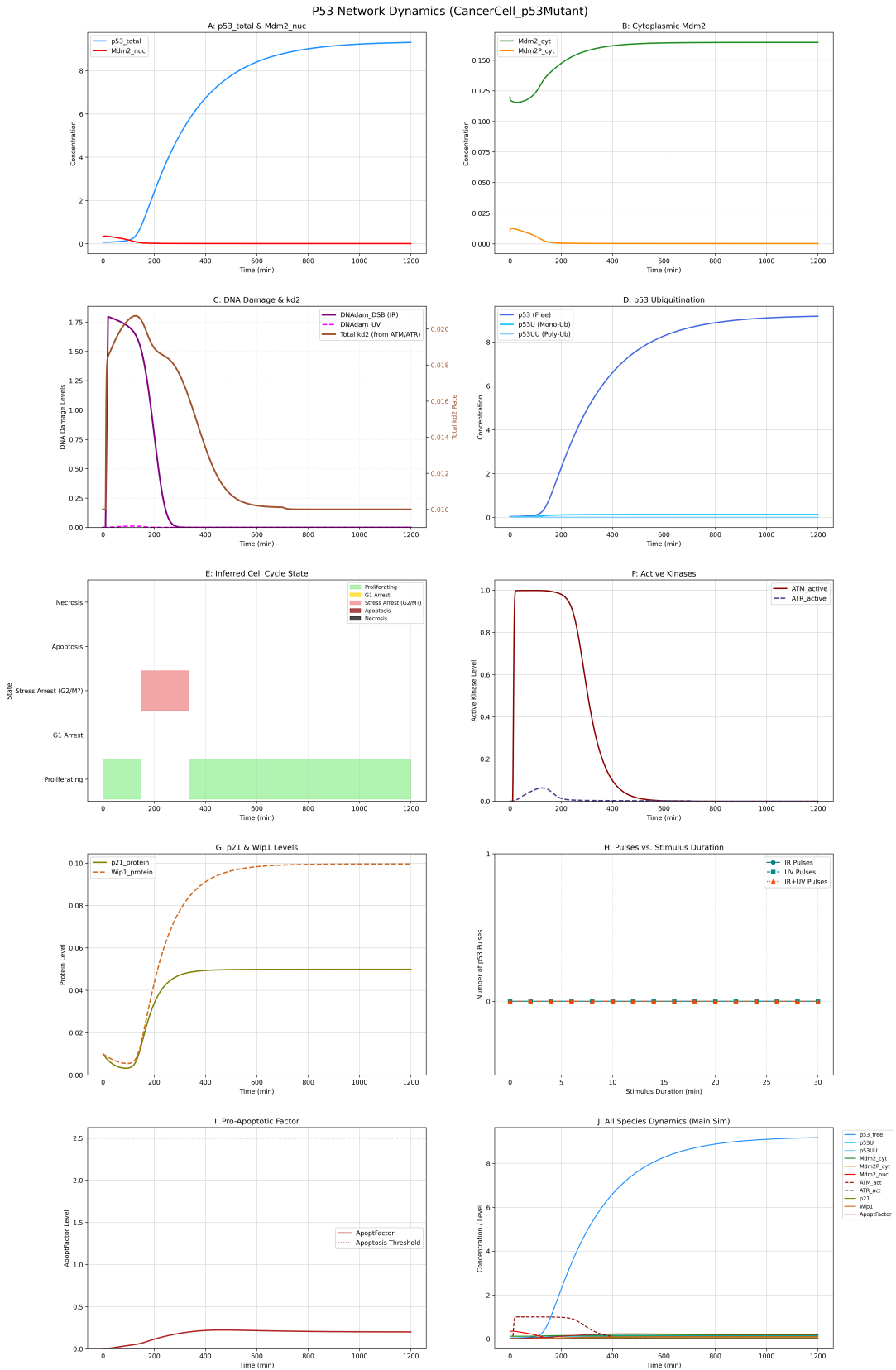


Figure 12: Cancer cell p53 mutant

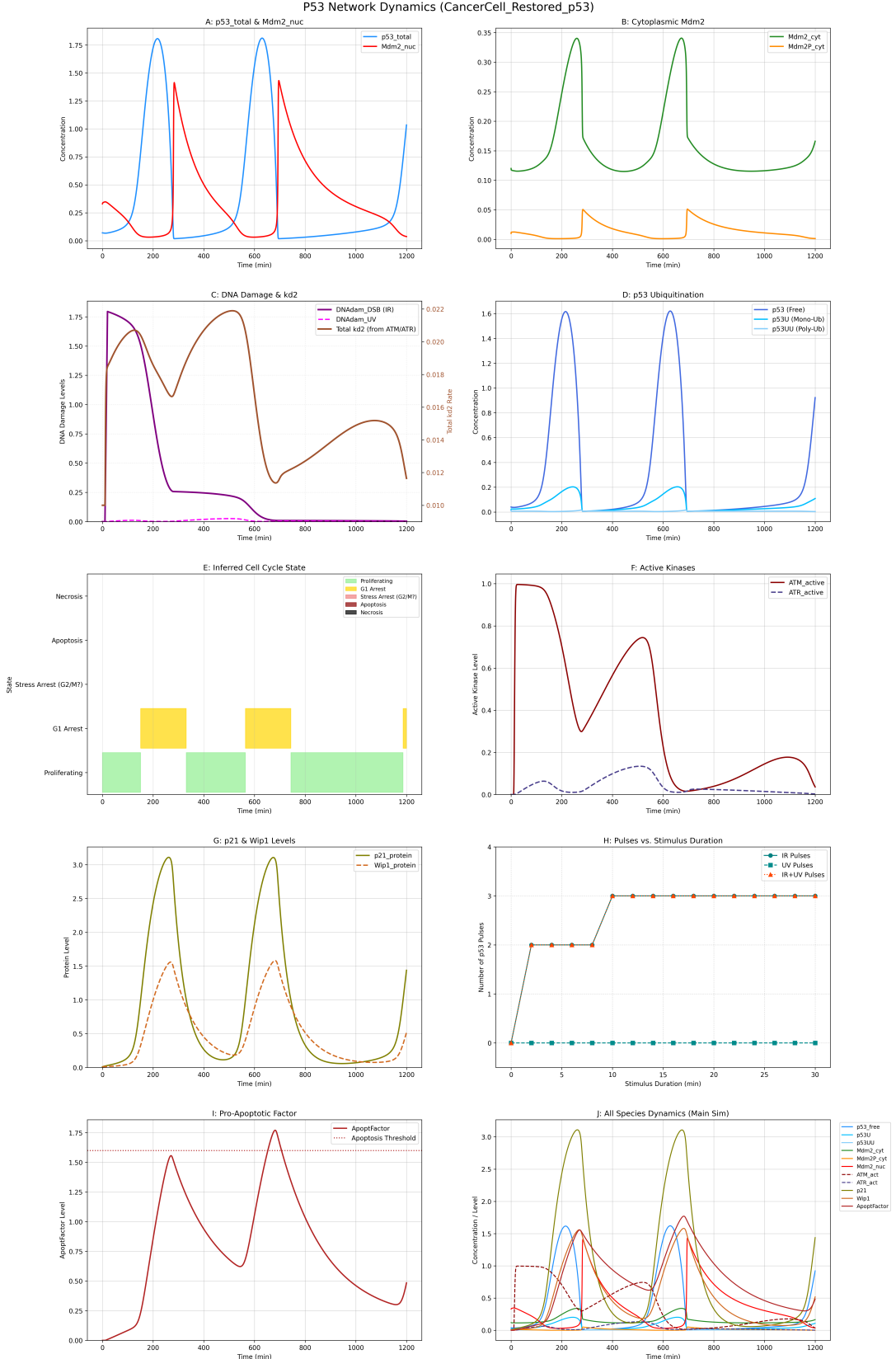


Figure 13: Cancer Cell p53 mutant - partially restored p53 dynamics (simulation of medical treatment)

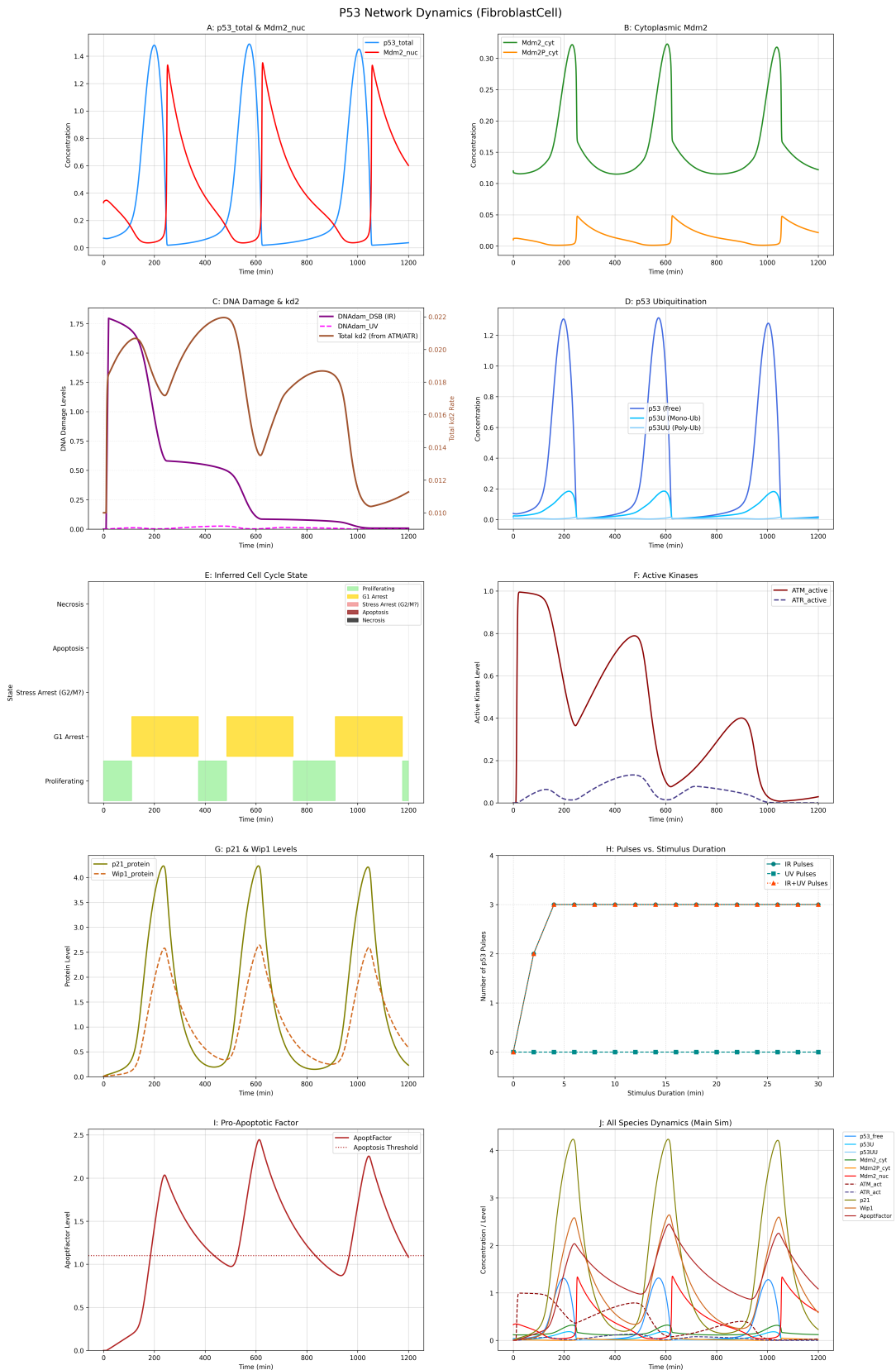


Figure 14: Fibroblast cell

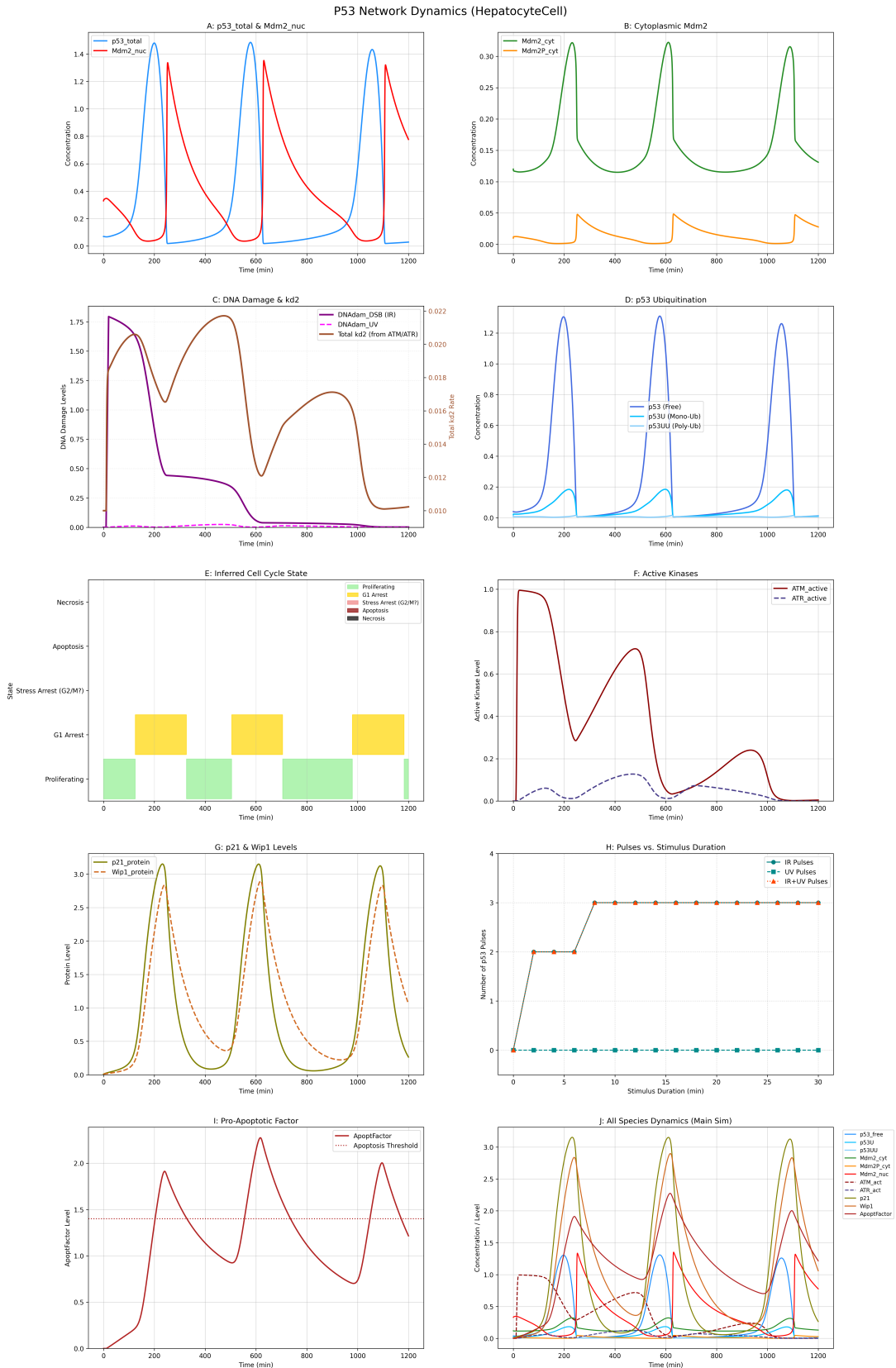


Figure 15: Hepatocyte Cell

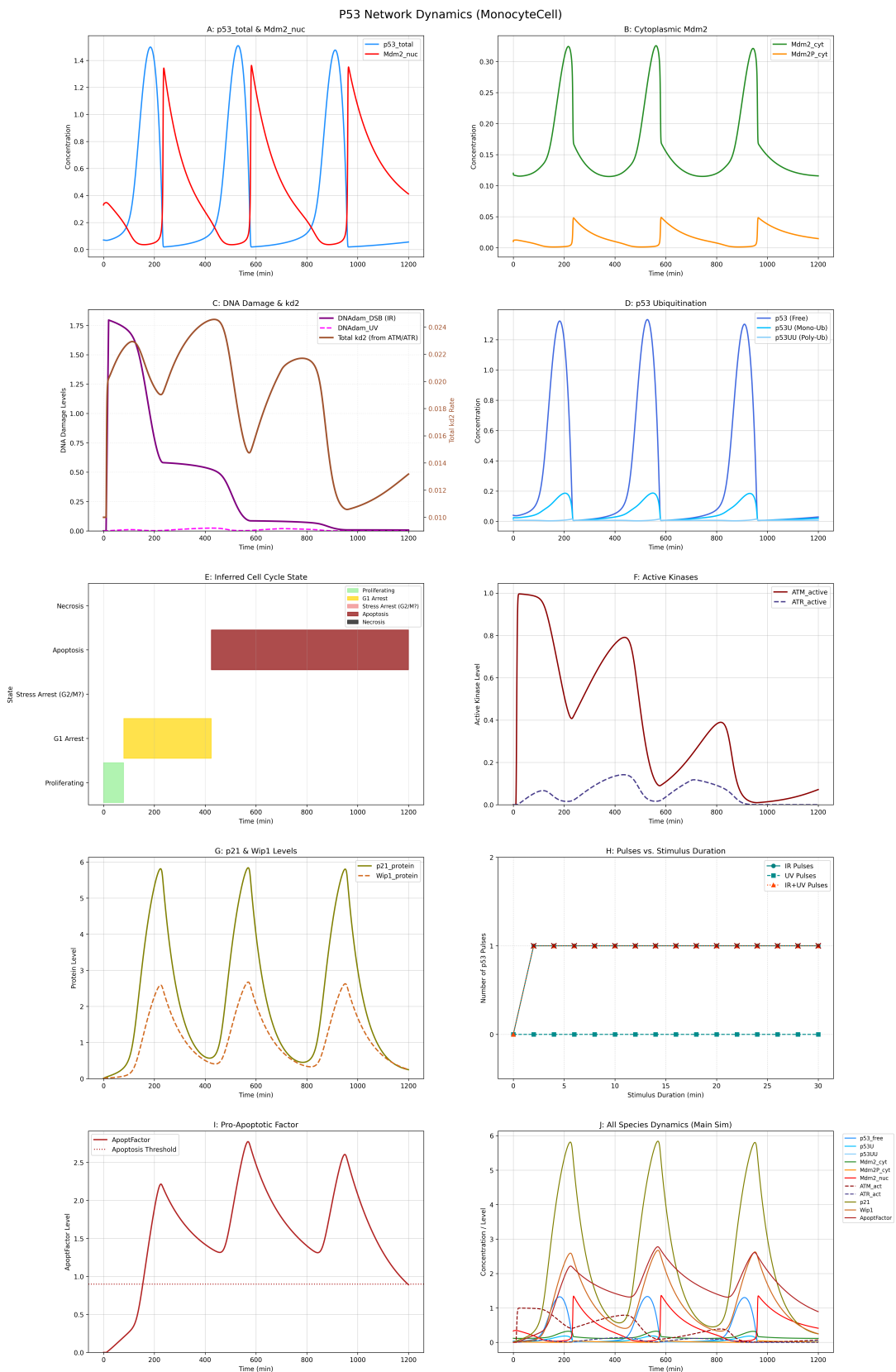


Figure 16: Monocyte Cell

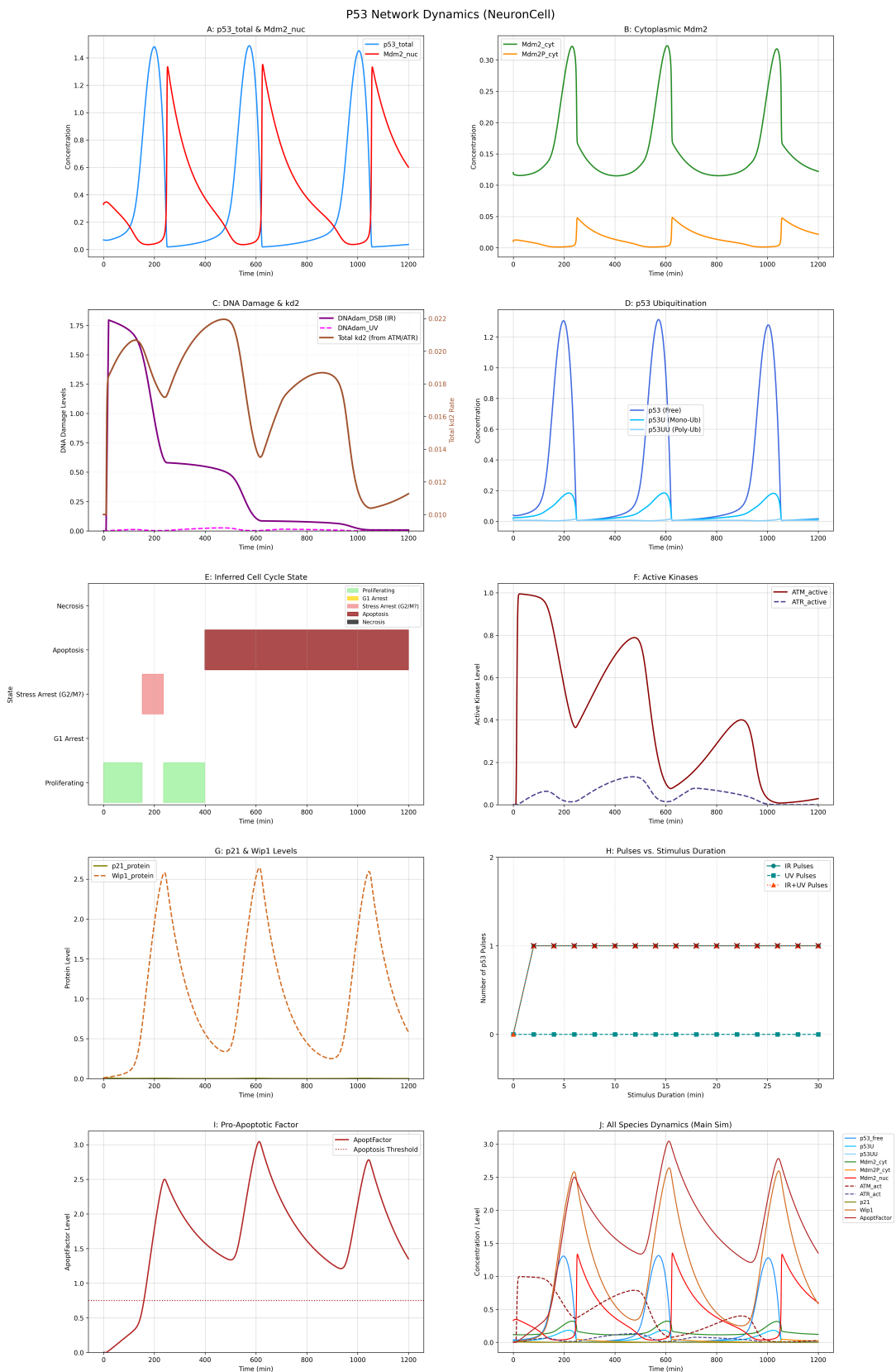


Figure 17: Neuron cell

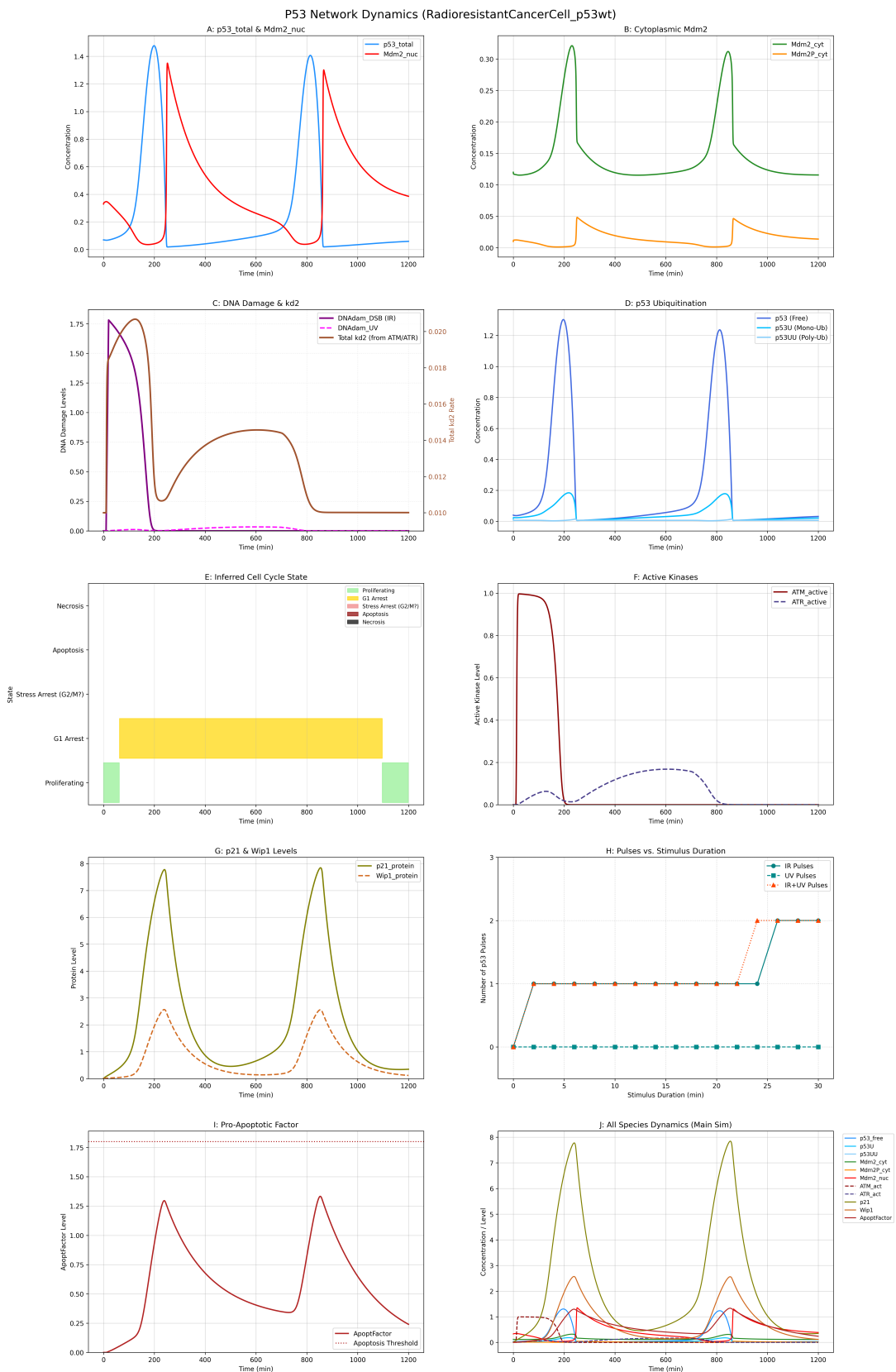


Figure 18: Radioresistant cell

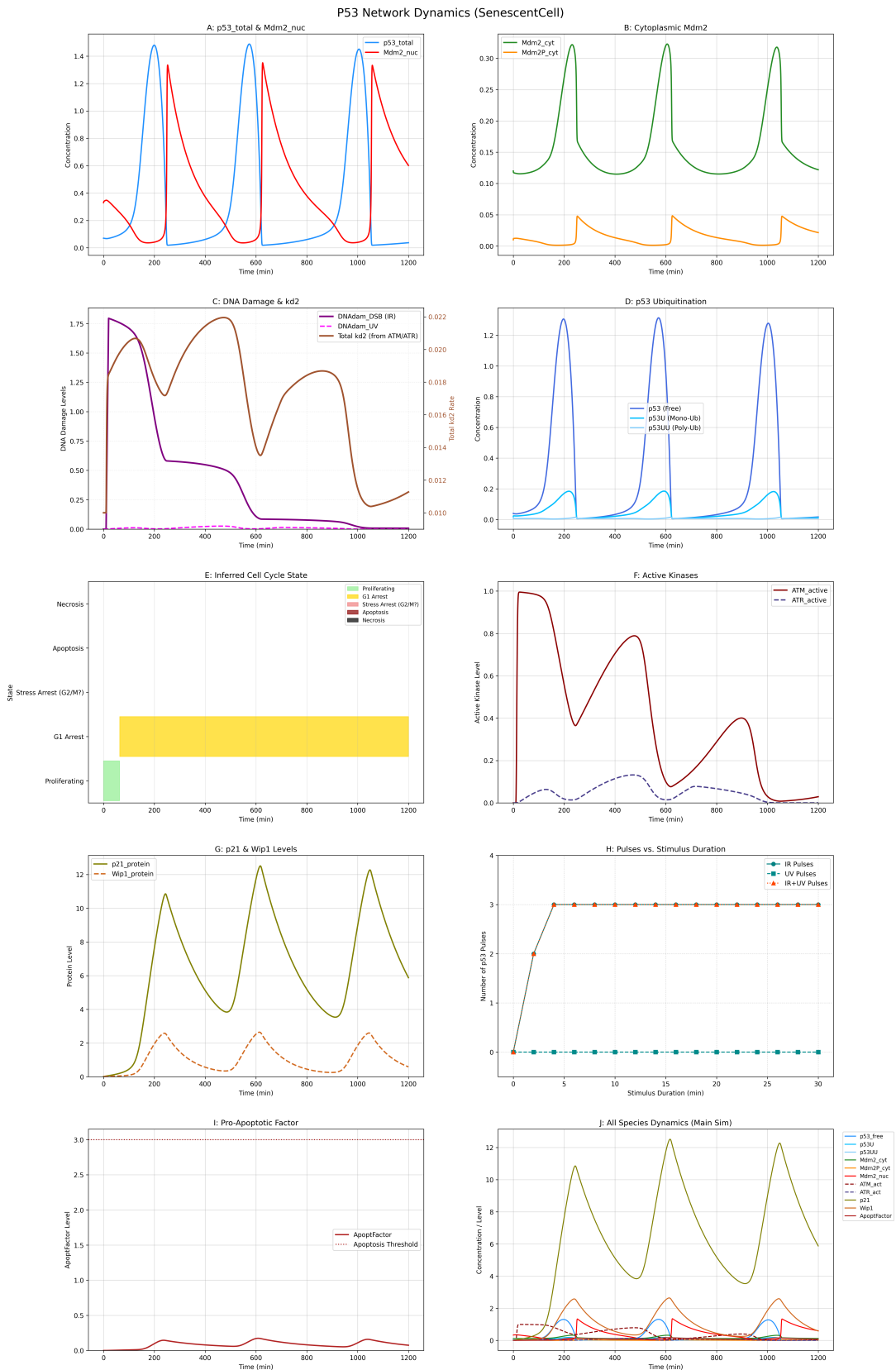


Figure 19: Senescent Cell

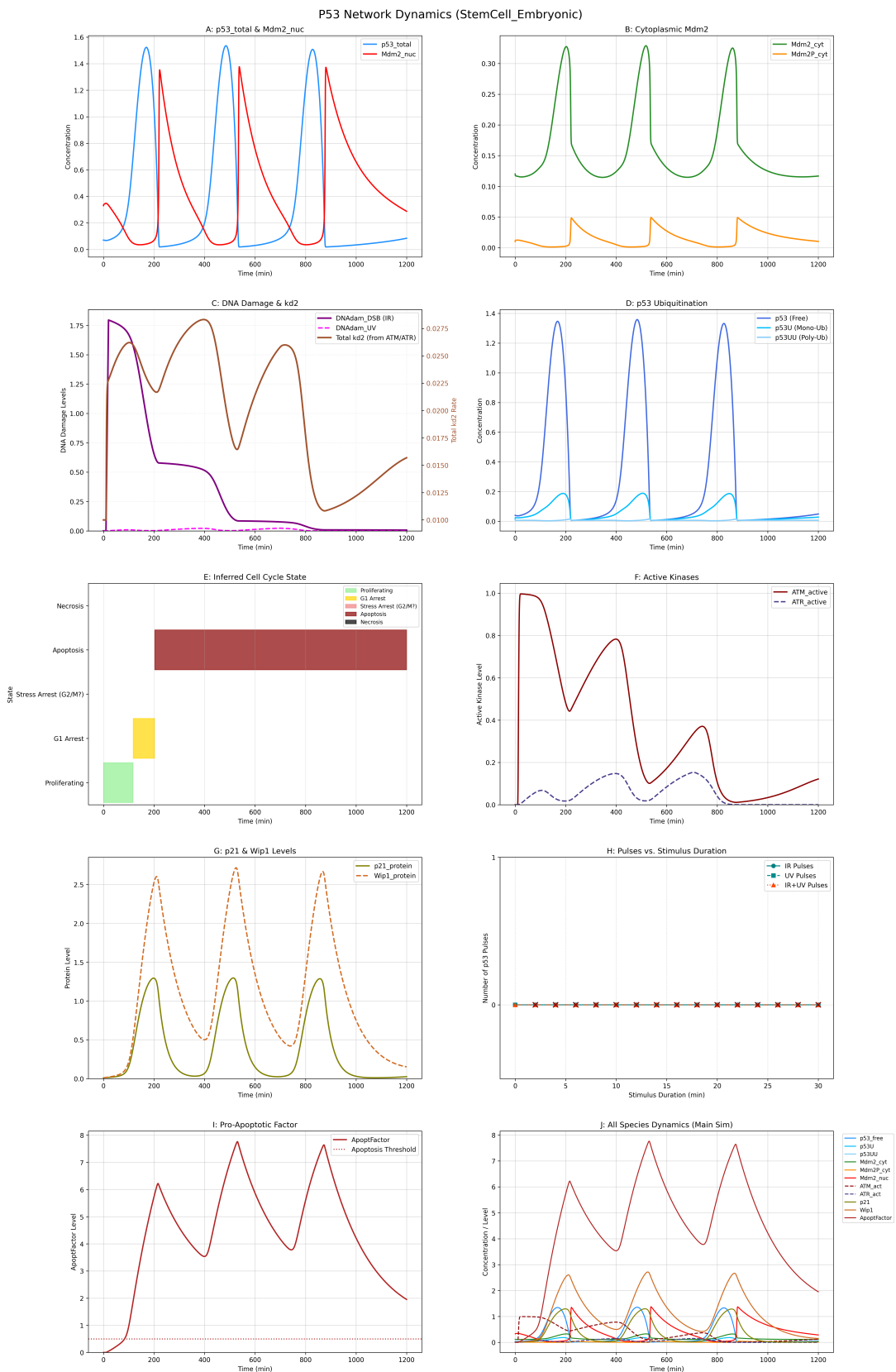


Figure 20: Stem Cell

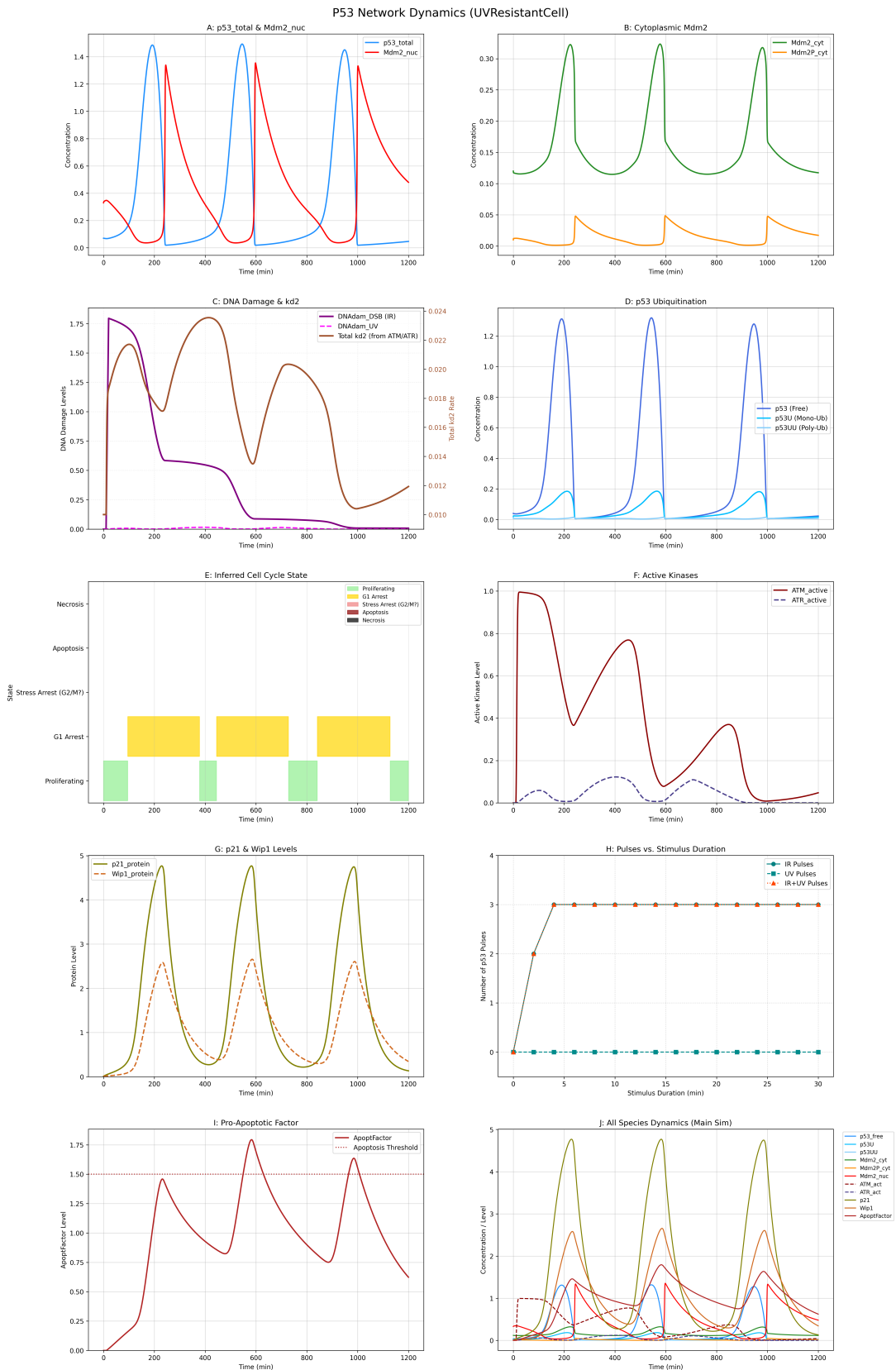


Figure 21: UV resistant cell

C Recreation of the Basic p53/Mdm2 Model by Ciliberto et al. (2005)

This section details the recreation of the core p53/Mdm2 network model as presented by Ciliberto, Novak, and Tyson in their 2005 paper, "Steady States and Oscillations in the p53/Mdm2 Network" [9]. The model captures the essential feedback loops between p53 and Mdm2, and their response to DNA damage induced by Ionizing Radiation (IR).

C.1 Model Species

The model tracks the concentrations of the following species:

- $[p53_{\text{tot}}]$: Total p53 protein
- $[p53U]$: Mono-ubiquitinated p53
- $[p53UU]$: Poly-ubiquitinated p53 (specifically di-ubiquitinated in the model's formulation, targeted for rapid degradation)
- $[Mdm2_{\text{cyt}}]$: Cytoplasmic Mdm2
- $[Mdm2P_{\text{cyt}}]$: Phosphorylated cytoplasmic Mdm2 (form capable of nuclear import)
- $[Mdm2_{\text{nuc}}]$: Nuclear Mdm2 (active in p53 ubiquitination)
- $[DNA_{\text{dam}}]$: Damaged DNA

An additional variable, $[p53]$, represents free, non-ubiquitinated p53 available for ubiquitination.

C.2 Auxiliary Equations

1. **Free p53:**

$$[p53] = \max(0, [p53_{\text{tot}}] - ([p53U] + [p53UU])) \quad (29)$$

2. **Damage-dependent Mdm2 nuclear degradation rate (k_{d2}):** The degradation rate of nuclear Mdm2 is enhanced by DNA damage:

$$k_{d2} = k'_{d2} + \frac{k''_{d2}[DNA_{\text{dam}}]}{J_{\text{dam}} + [DNA_{\text{dam}}]} \quad (30)$$

where k'_{d2} is the basal degradation rate and k''_{d2} is the maximum additional degradation rate due to damage.

3. **Ionizing Radiation (IR) Signal:** The DNA damage input is modeled as a pulse of ionizing radiation:

$$IR(t) = \begin{cases} ampl & \text{if } 10 < t < 20 \text{ (minutes)} \\ 0 & \text{otherwise} \end{cases} \quad (31)$$

C.3 Model Differential Equations

The dynamics of the system are described by the following set of ordinary differential equations (ODEs), as given in Table 1 of Ciliberto et al. (2005) [9]:

$$\frac{d[p53_{\text{tot}}]}{dt} = k_{s53} - k'_{d53}[p53_{\text{tot}}] - k_{d53}[p53UU] \quad (32)$$

$$\begin{aligned} \frac{d[p53U]}{dt} &= k_t[Mdm2_{\text{nuc}}][p53] + k_r[p53UU] \\ &\quad - [p53U](k_r + k_t[Mdm2_{\text{nuc}}]) - k'_{d53}[p53U] \end{aligned} \quad (33)$$

$$\frac{d[p53UU]}{dt} = k_t[Mdm2_{\text{nuc}}][p53U] - [p53UU](k_r + k'_{d53} + k_{d53}) \quad (34)$$

$$\frac{d[Mdm2_{\text{nuc}}]}{dt} = V_{\text{ratio}}(k_i[Mdm2P_{\text{cyt}}] - k_o[Mdm2_{\text{nuc}}]) - k_{d2}[Mdm2_{\text{nuc}}] \quad (35)$$

$$\begin{aligned} \frac{d[Mdm2_{\text{cyt}}]}{dt} &= k'_{s2} + \frac{k_{s2}[p53_{\text{tot}}]^m}{J_s^m + [p53_{\text{tot}}]^m} - k'_{d2}[Mdm2_{\text{cyt}}] \\ &\quad + k_{\text{deph}}[Mdm2P_{\text{cyt}}] - \frac{k_{\text{ph}}}{J_{\text{ph}} + [p53_{\text{tot}}]}[Mdm2_{\text{cyt}}] \end{aligned} \quad (36)$$

$$\begin{aligned} \frac{d[Mdm2P_{\text{cyt}}]}{dt} &= \frac{k_{\text{ph}}}{J_{\text{ph}} + [p53_{\text{tot}}]}[Mdm2_{\text{cyt}}] - k_{\text{deph}}[Mdm2P_{\text{cyt}}] - k_i[Mdm2P_{\text{cyt}}] \\ &\quad + k_o[Mdm2_{\text{nuc}}] - k'_{d2}[Mdm2P_{\text{cyt}}] \end{aligned} \quad (37)$$

$$\frac{d[DNA_{\text{dam}}]}{dt} = k_{\text{DNA}} \cdot IR(t) - k_{dDNA}[p53_{\text{tot}}] \frac{[DNA_{\text{dam}}]}{J_{\text{dna}} + [DNA_{\text{dam}}]} \quad (38)$$

A small constant ϵ (e.g., 10^{-9}) is typically added to denominators in computational implementations to prevent division by zero, though not explicitly shown in the original paper's equations.

C.4 Model Parameters

The parameter values used for simulation are taken from Table 2 of Ciliberto et al. (2005) [9]:

- $k'_{s2} = 0.0015 \text{ min}^{-1}$ (Basal Mdm2 synthesis rate)
- $k_{s2} = 0.006 \text{ min}^{-1}$ (p53-dependent Mdm2 synthesis rate)
- $k'_{d2} = 0.01 \text{ min}^{-1}$ (Basal Mdm2 degradation rate for all Mdm2 forms, and basal part of k_{d2})
- $k''_{d2} = 0.01 \text{ min}^{-1}$ (Coefficient for damage-dependent Mdm2 nuclear degradation; inferred interpretation from paper's Table 1, Table 2 and Fig 2C)
- $k_{\text{ph}} = 0.05 \text{ min}^{-1}$ (Mdm2 phosphorylation rate)
- $k_{\text{deph}} = 6 \text{ min}^{-1}$ (Mdm2P dephosphorylation rate)
- $k_i = 14 \text{ min}^{-1}$ (Mdm2P import rate to nucleus)
- $k_o = 0.5 \text{ min}^{-1}$ (Mdm2 export rate from nucleus)
- $k_{s53} = 0.055 \text{ min}^{-1}$ (p53 synthesis rate)
- $k_{d53} = 8 \text{ min}^{-1}$ (Degradation rate of $p53UU$)
- $k'_{d53} = 0.0055 \text{ min}^{-1}$ (Basal degradation rate for $p53_{\text{tot}}$, $p53U$, part of $p53UU$ degradation)
- $k_r = 8.8 \text{ min}^{-1}$ (Deubiquitination rate of $p53UU$ to $p53U$, and $p53U$ to $p53$)

- $k_t = 2.5 \text{ min}^{-1}$ (Ubiquitination rate of p53 by $Mdm2_{\text{nuc}}$)
- $k_{\text{DNA}} = 0.18 \text{ (damage units) min}^{-1}$ (DNA damage formation rate per unit IR signal)
- $k_{dDNA} = 0.017 \text{ min}^{-1}$ (p53-dependent DNA repair rate constant)
- $m = 3$ (Hill coefficient for Mdm2 synthesis by p53)
- $J_s = 1.2$ (Hill constant for Mdm2 synthesis by p53, concentration units)
- $J_{\text{ph}} = 0.01$ (Michaelis constant for Mdm2 phosphorylation denominator, concentration units)
- $J_{\text{dam}} = 0.2$ (Saturation constant for k_{d2} damage term, damage units)
- $J_{\text{DNA}} = 1$ (Saturation constant for DNA repair, damage units)
- $V_{\text{ratio}} = 15$ (Cytoplasmic to Nuclear volume ratio adjustment for nuclear Mdm2 concentration change)
- $ampl = 1$ (Amplitude of IR signal, dimensionless in this context)

Concentration units are arbitrary but consistent within the model. Time is in minutes.

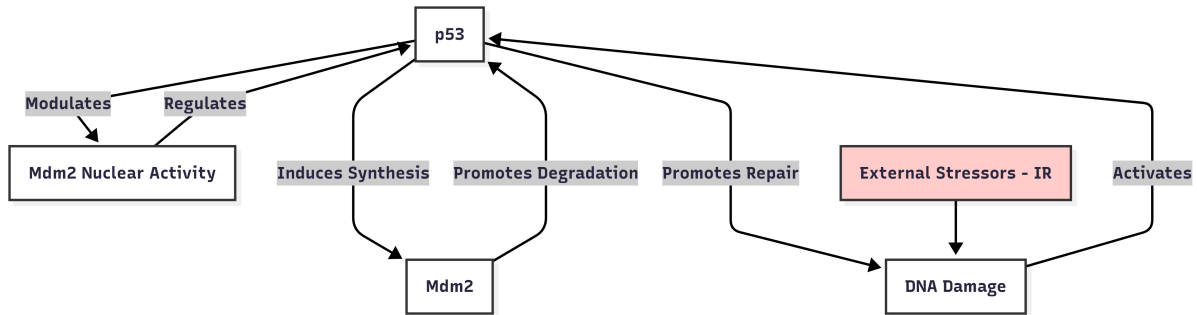


Figure 22: Diagram of basic model presented by Ciliberto, Novak, and Tyson in their 2005 paper, "Steady States and Oscillations in the p53/Mdm2 Network" [9].

C.5 Simulation Results

The model described above was implemented and simulated (using Python with the SciPy `solve_ivp` function). The simulation aims to reproduce the oscillatory dynamics observed in response to a pulse of DNA damage, as shown in Figure 2 of Ciliberto et al. (2005) [9].

Figure 23 shows that the simulation qualitatively reproduces the damped oscillations of total p53 and nuclear Mdm2. Following the IR pulse, DNA damage accumulates, leading to an increase in the nuclear degradation rate of Mdm2 (k_{d2}). This allows p53 to increase, which in turn induces Mdm2 synthesis (negative feedback) and promotes DNA repair. The interplay of these feedbacks results in oscillations that eventually dampen as DNA damage is repaired and the system returns to its low-p53 steady state.

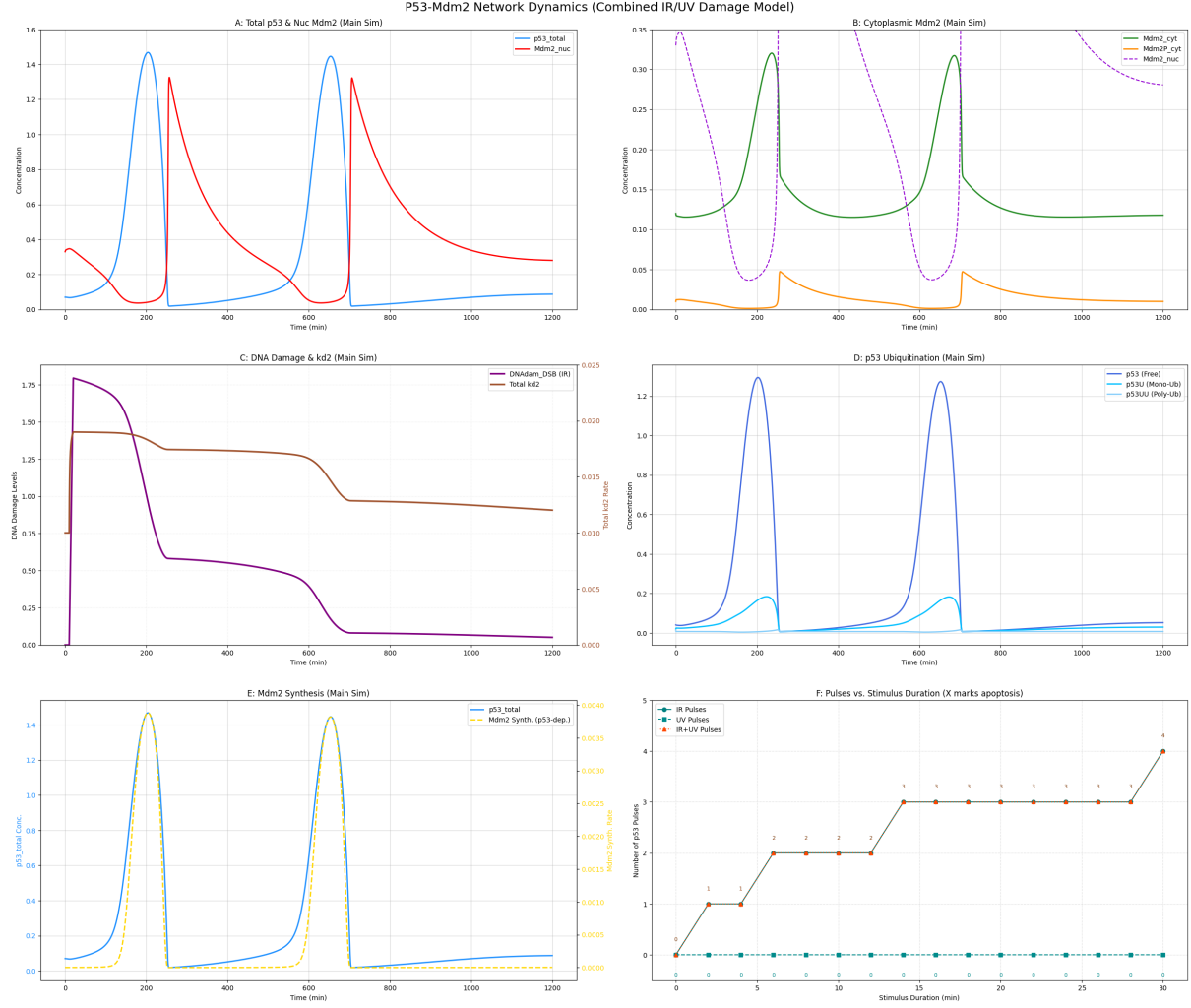


Figure 23: Recreation of p53/Mdm2 network dynamics following a pulse of IR-induced DNA damage (between $t=10$ and $t=20$ min), based on the model and parameters from Ciliberto et al. (2005). Panels should ideally show: (A) $[p53_{\text{tot}}]$ (solid line) and $[Mdm2_{\text{nuc}}]$ (dashed line). (B) Cytoplasmic Mdm2 forms ($[Mdm2_{\text{cyt}}]$, $[Mdm2P_{\text{cyt}}]$). (C) $[DNA_{\text{dam}}]$ (solid line) and the effective Mdm2 nuclear degradation rate k_{d2} (dashed line). This figure should be compared with Figure 2 in [9].

D Parameters of modeled Cells

Table 2: Full parameter set for the `AdvancedCell_Baseline` model. This serves as the reference for other cell type variants. Parameters are grouped by module/function.

Parameter Name (key)	Value	Description (Unit, Paper Ref. if Ciliberto)
p53 Dynamics		
ks53	0.055	Basal synthesis rate of total p53 (conc./min, C2005 T2)
kd53_	0.0055	Basal degradation rate of all p53 forms (min^{-1} , C2005 kd53')
kd53	8.0	Enhanced degradation of p53UU (min^{-1} , C2005 T2)
kf	8.8	Mdm2_nuc-p53 ubiquitination rate ((conc. min) $^{-1}$, C2005 kt)
kr	2.5	p53 de-ubiquitination rate (min^{-1} , C2005 T2)
Mdm2 Dynamics		
ks2_	0.0015	Basal Mdm2_cyt synthesis rate (conc./min, C2005 ks2')
ks2	0.006	Max p53-dependent Mdm2_cyt synthesis (conc./min, C2005 T2)
m	3	Hill coeff. for Mdm2 synthesis (dimless, C2005 T2)
Js	1.2	p53 for half-max Mdm2 synth. (conc., C2005 J_sm)
kph	0.05	Max Mdm2_cyt phosphorylation rate (conc./min, C2005 T2)
J	0.01	p53 for half-max Mdm2 phos. inhib. (conc., C2005 J_ph)
kdeph	6.0	Mdm2P_cyt dephosphorylation rate (min^{-1} , C2005 T2)
ki	14.0	Mdm2P_cyt nuclear import rate (min^{-1} , C2005 T2)
ko	0.5	Mdm2_nuc nuclear export rate (min^{-1} , C2005 T2)
Vratio	15.0	Volume ratio (Cytoplasm/Nucleus) (dimless, C2005 T2)
kd2_	0.01	Basal Mdm2 degradation rate (all forms) (min^{-1} , C2005 k'd2)
DSB (IR-like) Damage Parameters		
ampl_IR	1.0	Amplitude of IR signal (dimless, C2005 ampl)
IR_start	-1.0	IR exposure start time (min)
IR_end	-1.0	IR exposure end time (min)
kDNA_DSB	0.18	DNAAdam_DSB production rate by IR (DNAAdam/min per IR unit, C2005 kDNA)
kdDNA_DSB	0.017	p53-dep. DNAAdam_DSB repair rate ((conc. min) $^{-1}$ eff., C2005 kdDNA)
JDNA_DSB	1.0	Saturation for DNAAdam_DSB repair (DNAAdam conc., C2005 Jdna)
SSB (UV-like) Damage Parameters		
ampl_UV	1.0	Amplitude of UV signal (dimless)
UV_start	-1.0	UV exposure start time (min)
UV_end	-1.0	UV exposure end time (min)
kDNA_UV	0.15	DNAAdam_UV production rate by UV (DNAAdam/min per UV unit)
kdDNA_UV	0.035	p53-dep. DNAAdam_UV repair rate ((conc. min) $^{-1}$ eff.)
JDNA_UV	0.7	Saturation for DNAAdam_UV repair (DNAAdam conc.)
ATM Pathway (DSB response)		
ATM_total	1.0	Total ATM concentration (conc.)
k_act_atm_dsb	0.5	ATM activation rate by DNAAdam_DSB ((DNAAdam conc. min) $^{-1}$)
k_inact_atm_wip1	0.2	ATM_active inactivation by Wip1 ((Wip1 conc. min) $^{-1}$)
J_atm_kd2	0.2	Saturation for ATM_active on Mdm2_nuc deg. (ATM_active conc.)
kd2_ATM_max	0.01	Max add. Mdm2_nuc deg. by ATM_active (min^{-1})

Continued on next page

Table 2 – continued from previous page

Parameter Name (key)	Value	Description (Unit, Paper Ref. if Ciliberto)
ATR Pathway (SSB/stalled replication response)		
ATR_total	1.0	Total ATR concentration (conc.)
k_act_atr_uv	0.6	ATR activation rate by DNAdam_UV ((DNAdam conc. min) ⁻¹)
k_inact_atr	0.1	Basal ATR_active inactivation rate (min ⁻¹)
J_atr_kd2	0.2	Saturation for ATR_active on Mdm2_nuc deg. (ATR_active conc.)
kd2_ATR_max	0.01	Max add. Mdm2_nuc deg. by ATR_active (min ⁻¹)
p53-Mdm2 Interaction Modulation by Kinases		
K_inhibit_kf_atm	0.2	ATM_active for half-max kf inhibition (ATM_active conc.)
K_inhibit_kf_atr	0.2	ATR_active for half-max kf inhibition (ATR_active conc.)
p21 Dynamics (Cell Cycle Arrest)		
ks_p21	0.1	Max p21 synthesis rate by p53 (p21 conc./min)
J_p21	0.5	p53 for half-max p21 synthesis (p53 conc.)
h_p21	2	Hill coeff. for p21 synthesis (dimless)
kd_p21	0.02	p21 degradation rate (min ⁻¹)
Wip1 Dynamics (Negative Feedback on DDR)		
ks_wip1	0.05	Max Wip1 synthesis rate by p53 (Wip1 conc./min)
J_wip1	0.6	p53 for half-max Wip1 synthesis (p53 conc.)
h_wip1	2	Hill coeff. for Wip1 synthesis (dimless)
kd_wip1	0.01	Wip1 degradation rate (min ⁻¹)
Pro-Apoptotic Factor Dynamics		
ks_apopt	0.03	Max ApoptFactor synthesis by p53 (ApoptFactor conc./min)
J_apopt	0.8	p53 for half-max p53-driven ApoptFactor synth. (p53 conc.)
h_apopt	3	Hill coeff. for p53-driven ApoptFactor synth. (dimless)
ks_apopt_atm	0.002	Max ApoptFactor synthesis by ATM_active (ApoptFactor conc./min)
J_apopt_atm	0.1	ATM_active for half-max ATM-driven ApoptFactor synth. (ATM_active conc.)
ks_apopt_atr	0.002	Max ApoptFactor synthesis by ATR_active (ApoptFactor conc./min)
J_apopt_atr	0.1	ATR_active for half-max ATR-driven ApoptFactor synth. (ATR_active conc.)
kd_apopt	0.005	ApoptFactor degradation rate (min ⁻¹)
Interpretation Thresholds (Analysis)		
p53_tot_oscillation_threshold	0.5	Threshold for p53 oscillations (p53 conc.)
DNAdam_DSB_high_threshold	1.0	Threshold for "high" DSB damage (DNAdam_DSB conc.)
DNAdam_UV_high_threshold	1.0	Threshold for "high" UV damage (DNAdam_UV conc.)
ApoptFactor_threshold	1.0	ApoptFactor level for apoptosis trigger (ApoptFactor conc.)
ApoptFactor_duration_min	300	Min duration ApoptFactor above threshold (min)
p21_G1_arrest_threshold	0.4	p21 level for G1 arrest (p21 conc.)
p53_stress_arrest_threshold	0.8	p53_tot for stress arrest (p53 conc.)
ATM_active_stress_threshold	0.3	ATM_active for stress (ATM_active conc.)
ATR_active_stress_threshold	0.3	ATR_active for stress (ATR_active conc.)
DNAdam_DSB_necro_thresh	5.0	DNAdam_DSB for necrosis (DNAdam_DSB conc.)
DNAdam_UV_necro_thresh	6.0	DNAdam_UV for necrosis (DNAdam_UV conc.)
DNAdam_necro_duration_min	180	Min duration DNAdam for necrosis (min)
p53_apoptosis_duration_min	120	Min duration p53 above specific threshold (min)
p53_thresh_apopt_DSB	1.0	p53 for apoptosis if DSB dominant (p53 conc.)
p53_thresh_apopt_UV	1.2	p53 for apoptosis if UV dominant (p53 conc.)

Continued on next page

Table 2 – continued from previous page

Parameter Name (key)	Value	Description (Unit, Paper Ref. if Ciliberto)
p53_thresh_apopt_BOTH	0.8	p53 for apoptosis if both damage types (p53 conc.)
DNAAdam_DSB_apopt_thresh	1.5	DNAAdam_DSB for direct apoptosis (DNAAdam_DSB conc.)
DNAAdam_UV_apopt_thresh	2.0	DNAAdam_UV for direct apoptosis (DNAAdam_UV conc.)
DNAAdam_apopt_duration_min	200	Min duration high DNAAdam for direct apoptosis (min)

D.1 Parameter Modifications for UVResistantCell

Table 3: Parameter values for UVResistantCell that differ from AdvancedCell_Baseline (Table 2).

Parameter Name (key)	Baseline Value	UVResistantCell Value
kdDNA_UV	0.035	0.070
JDNA_UV	0.7	0.5
k_act_atr_uv	0.6	0.9
kd2__ATR_max	0.01	0.015
ks_p21	0.1	0.12
J_p21	0.5	0.4
ks_apopt	0.03	0.025
J_apopt	0.8	1.0
ApoptFactor_threshold	1.0	1.5
ApoptFactor_duration_min	300	360
p21_G1_arrest_threshold	0.4	0.35
ATR_active_stress_threshold	0.3	0.25

D.2 Parameter Modifications for MonocyteCell

Table 4: Parameter values for MonocyteCell that differ from AdvancedCell_Baseline (Table 2).

Parameter Name (key)	Baseline Value	MonocyteCell Value
K_inhibit_kf_atm	0.2	0.15
K_inhibit_kf_atr	0.2	0.15
k_act_atm_dsb	0.5	0.6
k_act_atr_uv	0.6	0.7
kd2__ATM_max	0.01	0.012
kd2__ATR_max	0.01	0.012
ks_p21	0.1	0.12
J_p21	0.5	0.4
kd_p21	0.02	0.015
p21_G1_arrest_threshold	0.4	0.3
ApoptFactor_threshold	1.0	0.9
ApoptFactor_duration_min	300	270
ks_apopt_atm	0.002	0.003
ks_apopt_atr	0.002	0.003
J_apopt_atm	0.1	0.08
J_apopt_atr	0.1	0.08

D.3 Parameter Modifications for CancerCellp53Mutant

Table 5: Parameter values for `CancerCellp53Mutant` that differ from `AdvancedCell_Baseline` (Table 2). Note: ks2 is based on baseline ks2_.

Parameter Name (key)	Baseline Value	CancerCellp53Mutant Value
ks2	0.006	0.00015
ks_p21	0.1	0.001
ks_wip1	0.05	0.001
ks_apopt	0.03	0.001
ApoptFactor_threshold	1.0	2.5
ApoptFactor_duration_min	300	600
ks_apopt_atm	0.002	0.0005
ks_apopt_atr	0.002	0.0005
p53_thresh_apopt_DSB	1.0	5.0
p53_thresh_apopt_UV	1.2	5.0
p53_thresh_apopt_BOTH	0.8	5.0
p21_G1_arrest_threshold	0.4	1.0

D.4 Parameter Modifications for StemCellEmbryonic

Table 6: Parameter values for `StemCellEmbryonic` that differ from `AdvancedCell_Baseline` (Table 2).

Parameter Name (key)	Baseline Value	StemCellEmbryonic Value
ks_apopt	0.03	0.06
J_apopt	0.8	0.3
h_apopt	3	4
ApoptFactor_threshold	1.0	0.5
ApoptFactor_duration_min	300	120
ks_apopt_atm	0.002	0.005
J_apopt_atm	0.1	0.05
ks_apopt_atr	0.002	0.005
J_apopt_atr	0.1	0.05
K_inhibit_kf_atm	0.2	0.1
K_inhibit_kf_atr	0.2	0.1
kd2__ATM_max	0.01	0.015
kd2__ATR_max	0.01	0.015
ks_p21	0.1	0.05
J_p21	0.5	0.6
kd_p21	0.02	0.03
k_act_atm_dsb	0.5	0.7
k_act_atr_uv	0.6	0.8

D.5 Parameter Modifications for SenescentCell

Table 7: Parameter values for `SenescentCell` that differ from `AdvancedCell_Baseline` (Table 2).

Parameter Name (key)	Baseline Value	SenescentCell Value
ks_p21	0.1	0.15
kd_p21	0.02	0.005
p21_G1_arrest_threshold	0.4	0.2
ks_apopt	0.03	0.005
J_apopt	0.8	1.5
ApoptFactor_threshold	1.0	3.0
ApoptFactor_duration_min	300	720
ks_apopt_atm	0.002	0.0001
ks_apopt_atr	0.002	0.0001

D.6 Parameter Modifications for CancerCellRestoredp53

Table 8: Parameter values for `CancerCellRestoredp53` that differ from its parent `CancerCellp53Mutant` (Table 5), with reference to `AdvancedCell_Baseline` (Table 2) values for restored parameters.

Parameter Name (key)	CancerMutant Value	Restored Value
ks2	0.00015	0.0045
ks_p21	0.001	0.075
ks_wip1	0.001	0.025
ks_apopt	0.001	0.018
ApoptFactor_threshold	2.5	1.6
ApoptFactor_duration_min	600	400
ks_apopt_atm	0.0005	0.001
ks_apopt_atr	0.0005	0.001
p53_thresh_apopt_DSB	5.0	1.2
p53_thresh_apopt_UV	5.0	1.4
p53_thresh_apopt_BOTH	5.0	1.0

D.7 Parameter Modifications for RadioresistantCancerCell

Table 9: Parameter values for `RadioresistantCancerCell` that differ from `AdvancedCell_Baseline` (Table 2).

Parameter Name (key)	Baseline Value	Radioresistant Value
kdDNA_DSB	0.017	0.040
JDNA_DSB	1.0	0.3
k_act_atm_dsb	0.5	0.65
ApoptFactor_threshold	1.0	1.8
ApoptFactor_duration_min	300	450
ks_apopt	0.03	0.02
ks_apopt_atm	0.002	0.001
ks_p21	0.1	0.15
J_p21	0.5	0.3
kd_p21	0.02	0.015
DNAAdam_DSB_necro_thresh	5.0	6.5

D.8 Parameter Modifications for FibroblastCell

Table 10: Parameter values for FibroblastCell that differ from AdvancedCell_Baseline (Table 2).

Parameter Name (key)	Baseline Value	FibroblastCell Value
p21_G1_arrest_threshold	0.4	0.35
ks_p21	0.1	0.11
J_p21	0.5	0.45
ApoptFactor_threshold	1.0	1.1
ApoptFactor_duration_min	300	330

D.9 Parameter Modifications for HepatocyteCell

Table 11: Parameter values for HepatocyteCell that differ from AdvancedCell_Baseline (Table 2).

Parameter Name (key)	Baseline Value	HepatocyteCell Value
kdDNA_DSB	0.017	0.020
kdDNA_UV	0.035	0.040
ApoptFactor_threshold	1.0	1.4
ApoptFactor_duration_min	300	350
ks_apopt	0.03	0.028
kd_p21	0.02	0.025
ks_wip1	0.05	0.055

D.10 Parameter Modifications for NeuronCell

Table 12: Parameter values for NeuronCell that differ from AdvancedCell_Baseline (Table 2).

Parameter Name (key)	Baseline Value	NeuronCell Value
ks_p21	0.1	0.0001
p21_G1_arrest_threshold	0.4	10.0
ApoptFactor_threshold	1.0	0.75
ApoptFactor_duration_min	300	240
ks_apopt	0.03	0.035
ks_apopt_atm	0.002	0.003
J_apopt_atm	0.1	0.08
ks_apopt_atr	0.002	0.003
J_apopt_atr	0.1	0.08
DNAAdam_DSB_necro_thresh	5.0	4.0
DNAAdam_necro_duration_min	180	120

D.11 Parameter Modifications for MelanocyteCell

Table 13: Parameter values for `MelanocyteCell` that differ from `AdvancedCell_Baseline` (Table 2).

Parameter Name (key)	Baseline Value	MelanocyteCell Value
kDNA_UV	0.15	0.13
k_act_atr_uv	0.6	0.75
ATR_total	1.0	1.1
kd2__ATR_max	0.01	0.013
kdDNA_UV	0.035	0.045
JDNA_UV	0.7	0.6
K_inhibit_kf_atr	0.2	0.15
ks_p21	0.1	0.11
J_p21	0.5	0.45
p21_G1_arrest_threshold	0.4	0.35
ApoptFactor_duration_min	300	280
ks_apopt_atr	0.002	0.0025
J_apopt_atr	0.1	0.09
p53_thresh_apopt_UV	1.2	1.0
p53_thresh_apopt_DSB	1.0	1.1
ks_wip1	0.05	0.055
DNAdam_UV_necro_thresh	6.0	5.0
DNAdam_necro_duration_min	180	150